



Measurement of beauty-strange meson production in Pb–Pb collisions at $\sqrt{s_{\text{NN}}} = 5.02$ TeV via non-prompt D_s^+ mesons

ALICE Collaboration*



ARTICLE INFO

Article history:

Received 25 May 2022

Received in revised form 7 October 2022

Accepted 8 November 2022

Available online 19 September 2023

Editor: M. Doser

Dataset link: <https://www.hepdata.net/record/ins2071181>

ABSTRACT

The production yields of non-prompt D_s^+ mesons, namely D_s^+ mesons from beauty-hadron decays, were measured for the first time as a function of the transverse momentum (p_T) at midrapidity ($|y| < 0.5$) in central and semi-central Pb–Pb collisions at a centre-of-mass energy per nucleon pair $\sqrt{s_{\text{NN}}} = 5.02$ TeV with the ALICE experiment at the LHC. The D_s^+ mesons and their charge conjugates were reconstructed from the hadronic decay channel $D_s^+ \rightarrow \phi \pi^+$, with $\phi \rightarrow K^- K^+$, in the $4 < p_T < 36$ GeV/c and $2 < p_T < 24$ GeV/c intervals for the 0–10% and 30–50% centrality classes, respectively. The measured yields of non-prompt D_s^+ mesons are compared to those of prompt D_s^+ and non-prompt D^0 mesons by calculating the ratios of the production yields in Pb–Pb collisions and the nuclear modification factor R_{AA} . The ratio between the R_{AA} of non-prompt D_s^+ and prompt D_s^+ mesons, and that between the R_{AA} of non-prompt D_s^+ and non-prompt D^0 mesons in central Pb–Pb collisions are found to be on average higher than unity in the $4 < p_T < 12$ GeV/c interval with a statistical significance of about 1.6σ and 1.7σ , respectively. The measured R_{AA} ratios are compared with the predictions of theoretical models of heavy-quark transport in a hydrodynamically expanding QGP that incorporate hadronisation via quark recombination.

© 2022 The Author(s). Published by Elsevier B.V. This is an open access article under the CC BY license (<http://creativecommons.org/licenses/by/4.0/>). Funded by SCOAP³.

1. Introduction

A transition from ordinary nuclear matter to a colour-deconfined medium called quark-gluon plasma (QGP) is predicted to occur at a very high temperature and energy density by quantum chromodynamics (QCD) calculations on the lattice [1–3], and is supported by several measurements in ultrarelativistic heavy-ion collisions at the SPS, RHIC, and LHC [4–11]. In such collisions, charm and beauty quarks are mainly produced in hard scattering processes that occur before the formation of the QGP. Hence, they are effective probes of the entire system evolution. While the system undergoes a hydrodynamic expansion, they interact with the medium constituents via elastic [12–14] and inelastic [15,16] scatterings. These interactions imply that charm and beauty quarks exchange energy and momentum with the medium constituents, causing high-momentum quarks to lose part of their energy while traversing the QGP. The in-medium energy loss is commonly studied via the measurement of the nuclear modification factor,

$$R_{\text{AA}}(p_T) = \frac{1}{\langle T_{\text{AA}} \rangle} \times \frac{dN_{\text{AA}}/dp_T}{d\sigma_{\text{pp}}/dp_T}, \quad (1)$$

where dN_{AA}/dp_T is the transverse-momentum (p_T) differential production yield in nucleus–nucleus collisions, $d\sigma_{\text{pp}}/dp_T$ the p_T -

differential cross section in proton–proton (pp) collisions, and $\langle T_{\text{AA}} \rangle$ is the average of the nuclear overlap function [17]. Several measurements of charm and beauty hadrons in Pb–Pb [18–30] and Au–Au [31–33] collisions show a strong suppression of the production yield at intermediate and high p_T ($p_T > 4–5$ GeV/c) in heavy-ion collisions compared to pp collisions, suggesting a substantial energy loss of heavy quarks in the QGP. The comparison of the R_{AA} of light, charm, and beauty hadrons indicates that the energy loss is sensitive to the colour charge and the parton mass. In particular, the R_{AA} of beauty hadrons is observed to be larger than that of charm hadrons [21,24]. For $p_T > 5–6$ GeV/c, where radiative processes are expected to dominate the energy loss, the smaller suppression is attributed mainly to the so-called “dead cone” effect [34,35], which suppresses the gluon radiation at angles smaller than $\theta \approx m_Q/E_Q$, where m_Q is the mass of the quark and E_Q its energy.

Instead, low- p_T heavy quarks experience a “Brownian motion”, which consists of a diffusion process occurring via multiple elastic interactions with low-momentum transfer [36]. Owing to the larger mass, beauty quarks diffuse less than charm quarks and have a longer relaxation time, which is expected to be proportional to the quark mass. Measurements of the heavy-flavour hadron production and azimuthal anisotropies can be exploited to constrain the spatial diffusion coefficient D_s via the comparison with theoretical models based on the heavy-quark transport in a hydrodynamically expanding QGP [18,37].

* E-mail address: alice-publications@cern.ch.

A precise description of the hadronisation process in the hot nuclear matter is crucial to understand the transport properties of the QGP [38]. The hadronisation mechanism of low and intermediate- p_T heavy quarks is expected to be sensitive to the presence of a colour-deconfined medium, which could enable hadron formation via quark recombination in addition to the vacuum-like fragmentation. This leads to an enhancement of the production yield of heavy-flavour hadrons with strange-quark content relative to those of non-strange hadrons in Pb–Pb collisions compared to pp collisions, caused by the abundant production of strange-antistrange quark pairs in the QGP [11,39,40]. Recent measurements of the production of prompt D_s^+ mesons, i.e. D_s^+ mesons originating from the charm-quark hadronisation or decays of excited charm-hadron states, by the STAR [41] and ALICE [19,42] Collaborations suggest a relevant role of the recombination mechanism in the charm-quark hadronisation. Similar studies in the open-beauty sector, conducted by the CMS Collaboration via the measurement of the B_s^0 -meson production relative to that of B^+ mesons, show a hint of enhanced production of strange over non-strange mesons [26,43]. However, no firm conclusions can be drawn within the current uncertainties. Complementary information about the heavy-quark hadronisation in presence of the medium is provided by the measurements of charm baryons and charmonia in heavy-ion collisions [20,27,44–47]. Recently, the production of heavy-flavour hadrons containing strange quarks was also investigated in high-multiplicity pp collisions [48,49], following the observation of an enhanced production of strange and multi-strange hadrons with increasing charged-particle multiplicity in the light-flavour sector [50].

In this Letter, the measurement of the production of D_s^+ mesons originating from beauty-hadron decays (non-prompt) is reported for central (0–10%) and semicentral (30–50%) Pb–Pb collisions at a centre-of-mass energy per nucleon pair $\sqrt{s_{NN}} = 5.02$ TeV. Non-prompt D_s^+ mesons provide information about the diffusion and the energy loss of beauty quarks in the QGP. In addition, together with the measurement of non-prompt D^0 mesons, they have the potential to reveal the beauty-quark hadronisation mechanisms in the QGP, since in pp collisions about 50% of non-prompt D_s^+ mesons are produced in B_s^0 decays [51,52]. Therefore, the non-prompt D_s^+ p_T -differential production yield and R_{AA} are compared with those of prompt D_s^+ and non-prompt D^0 mesons, as well as with theoretical models based on beauty-quark transport in the QGP.

2. Experimental apparatus and analysis technique

The D_s^+ -mesons were reconstructed from their hadronic decays with the ALICE central barrel detectors, which cover the full azimuth in the pseudorapidity interval $|\eta| < 0.9$ and are embedded in a large solenoidal magnet providing a uniform 0.5 T magnetic field parallel to the beam direction. Charged-particle trajectories are reconstructed from their hits in the Inner Tracking System (ITS) [53] and the Time Projection Chamber (TPC) [54]. Particle identification (PID) is provided via the measurement of the specific ionisation energy loss dE/dx in the TPC and of the flight time of the particles from the interaction point to the Time-Of-Flight detector (TOF) [55]. The reconstruction of the interaction vertex and of the decay vertices of charm- and beauty-hadron decays relies on the precise determination of the track parameters in the vicinity of the interaction point provided by the ITS.

The data sample of Pb–Pb collisions used in the analysis was collected with the ALICE detector in 2018, during LHC Run 2. Three trigger classes were considered: minimum bias, central, and semicentral, all based on the signals in the two scintillator arrays of the VO detector [56], which covers the full azimuth in the pseudorapidity intervals $-3.7 < \eta < -1.7$ (VOC) and $2.8 < \eta < 5.1$ (VOA).

Background events due to the interaction of one of the beams with residual gas in the vacuum tube and other machine-induced backgrounds were rejected offline using the timing information provided by the V0 and the neutron Zero Degree Calorimeters (ZDC) [57]. Only events with a primary vertex reconstructed within ± 10 cm from the centre of the detector along the beam-line direction were considered in the analysis. Collisions were classified into centrality intervals, defined in terms of percentiles of the hadronic Pb–Pb cross section, based on the V0 signal amplitude as described in detail in Ref. [58]. The measurement of non-prompt D_s^+ -meson production was carried out for central (0–10%) and semicentral (30–50%) collisions. The number of events considered for the analysis is about 100×10^6 and 85×10^6 in the 0–10% and 30–50% centrality intervals, corresponding to integrated luminosities \mathcal{L}_{int} of $(130.5 \pm 0.5) \mu\text{b}^{-1}$ and $(55.5 \pm 0.2) \mu\text{b}^{-1}$, respectively [59]. The average values of the nuclear overlap function, $\langle T_{AA} \rangle$, for the considered central and semicentral event intervals were estimated via Glauber-model [60] simulations anchored to the V0 signal amplitude distribution, and are $(23.26 \pm 0.17) \text{ mb}^{-1}$ and $(3.92 \pm 0.06) \text{ mb}^{-1}$ [17,59], respectively.

The D_s^+ mesons and their charge conjugates were reconstructed via the $D_s^+ \rightarrow \phi\pi^+ \rightarrow K^-K^+\pi^+$ decay channel with branching ratio $\text{BR} = (2.24 \pm 0.08)\%$ [51]. The analysis was based on the reconstruction of decay-vertex topologies displaced from the interaction vertex. For prompt mesons, the separation between the interaction point and the D_s^+ decay vertex is governed by the mean proper decay length $c\tau$ of D_s^+ mesons, which is about 151 μm [51]. The decay vertices of non-prompt D_s^+ mesons on average are more displaced than those of prompt D_s^+ mesons due to the large mean proper decay lengths of beauty hadrons ($c\tau \simeq 450 \mu\text{m}$ [51]). Therefore, by exploiting the selection of displaced decay-vertex topologies, it is possible to separate non-prompt D_s^+ mesons from the combinatorial background and from prompt D_s^+ mesons.

D_s^+ -meson candidates were built combining triplets of tracks with the proper charge signs, each with $|\eta| < 0.8$, at least 70 (out of a maximum of 159) crossed TPC pad rows, a track fit quality $\chi^2/\text{ndf} < 1.25$ in the TPC (where ndf is the number of degrees of freedom involved in the track fit procedure), and a minimum of two (out of a maximum of six) hits in the ITS, with at least one in either of the two innermost layers, which provide the best pointing resolution. Moreover, at least 50 clusters available for particle identification in the TPC were required, and only tracks with p_T above 0.6 (0.4) GeV/c were considered for central (semicentral) collisions. These track selection criteria limit the D_s^+ -meson acceptance in rapidity, which drops steeply to zero for $|y| > 0.5$ at low p_T and for $|y| > 0.8$ at $p_T > 5 \text{ GeV}/c$. Thus, only D_s^+ -meson candidates within a p_T -dependent fiducial acceptance region, $|y| < y_{\text{fid}}(p_T)$, were selected. The $y_{\text{fid}}(p_T)$ value was defined as a second-order polynomial function, increasing from 0.5 to 0.8 in the transverse-momentum range $0 < p_T < 5 \text{ GeV}/c$, and as a constant term, $y_{\text{fid}} = 0.8$, for $p_T > 5 \text{ GeV}/c$.

Similarly to other recent D-meson measurements by the ALICE Collaboration [19,21,52], Boosted Decision Trees (BDT) algorithms were employed to reduce the large combinatorial background and to separate the contribution of prompt and non-prompt D_s^+ mesons through a multiclass classification. In particular, the implementation of the BDT algorithm provided by the XGBoost [61,62] library was used. Background samples for the BDT training were extracted from the sidebands of the candidate invariant mass distributions in the data, namely from the $1.72 < M(\text{KK}\pi) < 1.83 \text{ GeV}/c^2$ and $2.01 < M(\text{KK}\pi) < 2.12 \text{ GeV}/c^2$ regions. Applying these selections, candidates belonging to $D^+ \rightarrow K^-K^+\pi^+$ decays are rejected. Signal samples of prompt and non-prompt D_s^+ mesons were obtained from Monte Carlo (MC) simulations. The MC samples were built by simulating Pb–Pb collisions with the HIJING 1.36 [63] event generator in order to describe the charged-

particle multiplicity and detector occupancy. To enrich the sample of prompt and non-prompt D-meson signals, additional $c\bar{c}$ - and $b\bar{b}$ -quark pairs were injected into each HIJING event using the PYTHIA 8.243 event generator [64,65] with Monash tune [66]. The D_s^+ mesons were forced to decay into the hadronic channel of interest for the analysis. The generated particles were then propagated through the apparatus using the GEANT3 transport code [67]. Detailed descriptions of the detector response, the geometry of the apparatus and the conditions of the luminous region, including their evolution with time during the data taking period, were included in the simulation. Before the BDT training, loose kinematic and topological selections were applied to the D_s^+ -meson candidates together with the particle identification of decay-product tracks. The D_s^+ -meson candidate information provided to the BDTs, as an input for the models to distinguish among prompt and non-prompt mesons and background candidates, was mainly based on the displacement of the tracks from the primary vertex, the distance between the D_s^+ -meson decay vertex and the primary vertex, the D_s^+ -meson impact parameter, and the cosine of the pointing angle between the D_s^+ -meson candidate line of flight (the vector connecting the primary and secondary vertices) and its reconstructed momentum vector. In addition, the absolute difference between the reconstructed K^+K^- invariant mass and the PDG average mass for the ϕ meson [51] and variables related to the PID of decay tracks were also included. Independent BDTs were trained in the different p_T intervals of the analysis and for the different centrality intervals. Subsequently, they were applied to the real data sample in which the type of candidate is unknown. The BDT outputs are related to the candidate probability to be a non-prompt D_s^+ meson or combinatorial background. Selections on the BDT outputs were optimised to obtain a high non-prompt D_s^+ -meson fraction while maintaining a reliable signal extraction from the candidate invariant mass distributions.

The D_s^+ -meson candidates were selected by requiring a high probability to be non-prompt D_s^+ mesons and a low probability to be combinatorial background. The raw yield of D_s^+ mesons, including both particles and antiparticles, was extracted from binned maximum-likelihood fits to the invariant mass (M) distributions in transverse-momentum intervals $4 < p_T < 36 \text{ GeV}/c$ and $2 < p_T < 24 \text{ GeV}/c$ for the 0–10% and the 30–50% centrality intervals, respectively. The fit function was composed of a Gaussian for the description of the signal and an exponential term for the background. An additional Gaussian was used to describe the peak due to the decay $D^+ \rightarrow K^-K^+\pi^+$, with a branching ratio of $(9.68 \pm 0.18) \times 10^{-3}$ [51], present at a lower invariant mass value than the D_s^+ -meson signal peak. To improve the stability of the fits, the width of the D_s^+ -meson signal peak was fixed to the value extracted from a data sample dominated by prompt candidates, which is characterised by a signal extraction with higher statistical significance. As an example, the invariant mass distribution for the $4 < p_T < 6 \text{ GeV}/c$ interval in central Pb–Pb collisions, together with the result of the fit and the estimated non-prompt fraction is reported in Fig. 1. The measured raw yield, although dominated by non-prompt candidates, still contains a residual contribution of prompt D_s^+ mesons which satisfy the BDT-based selections. The procedure used to calculate the fraction of non-prompt candidates present in the extracted raw yield is described below. The statistical significance of the observed signals varies from about 4 to 11 depending upon the p_T and centrality intervals.

The corrected p_T -differential yields of non-prompt D_s^+ mesons were computed for each p_T interval as

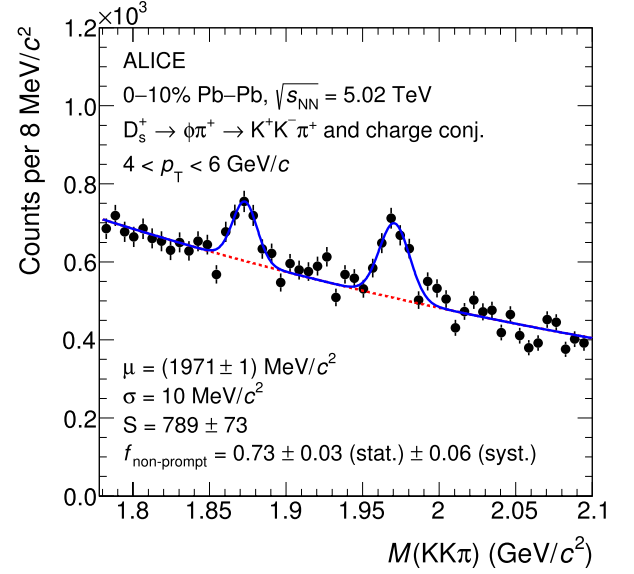


Fig. 1. Invariant mass distribution of non-prompt D_s^+ candidates and their charge conjugates in the $4 < p_T < 6 \text{ GeV}/c$ interval for central Pb–Pb collisions. The blue solid line shows the total fit function and the red dashed line the combinatorial-background contribution. The values of the mean (μ), width (σ), and raw yield (S) of the signal peak are reported together with their statistical uncertainties resulting from the fit. The fraction of non-prompt candidates in the measured raw yield is reported with its statistical and systematic uncertainties.

$$\frac{dN}{dp_T} \Big|_{|y|<0.5} = \frac{1}{2} \times \frac{1}{\Delta p_T} \\ \times \frac{f_{\text{non-prompt}}(p_T) \times N^{D+\bar{D},\text{raw}}(p_T)}{c_{\Delta y}(p_T) \times (\text{Acc} \times \varepsilon)_{\text{non-prompt}}(p_T) \times \text{BR} \times N_{\text{evt}}} . \quad (2)$$

The raw-yield values $N^{D+\bar{D},\text{raw}}$ were divided by a factor of two and multiplied by the non-prompt fraction $f_{\text{non-prompt}}$ to obtain the charge-averaged yields of non-prompt D_s^+ mesons. Furthermore, they were divided by the acceptance-times-efficiency correction factor of non-prompt D_s^+ mesons $(\text{Acc} \times \varepsilon)_{\text{non-prompt}}$, the BR of the decay channel, the width of the p_T interval Δp_T , the correction factor for the rapidity coverage $c_{\Delta y}$, and the number of analysed events N_{evt} . The correction factor for the rapidity acceptance $c_{\Delta y}$ was defined as the ratio between the generated D-meson yield in $\Delta y = 2 y_{\text{fid}}(p_T)$ and that in $|y| < 0.5$. It was computed with FONLL perturbative QCD calculations [68,69] as in Refs. [18,19].

The $(\text{Acc} \times \varepsilon)$ correction factor was obtained from MC simulations, using samples not employed in the BDT training. The D_s^+ -meson p_T distributions from simulations were reweighed in order to mimic the realistic shapes in the determination of the $(\text{Acc} \times \varepsilon)$ factor, which depends on p_T . In particular, weights were applied to the p_T distributions of prompt D_s^+ mesons and of beauty-hadron mother particles in case of non-prompt D_s^+ mesons. These weights were defined to reproduce the shapes given by FONLL calculations multiplied by the R_{AA} of prompt D_s^+ mesons and B mesons predicted by the TAMU [70,71] model. The TAMU model implements the charm- and beauty-quark transport inside a strangeness-rich QGP, and it reasonably reproduces the prompt D-meson measurements at low p_T [18,19]. The $(\text{Acc} \times \varepsilon)$ factors as a function of p_T for prompt and non-prompt D_s^+ mesons in the 0–10% and 30–50% centrality intervals are displayed in Fig. 2, along with the ratios of the non-prompt to prompt factors. The prompt D_s^+ -meson acceptance times efficiency is smaller than that of non-prompt D_s^+ mesons by a factor varying from 5 to 20 depending on p_T and centrality. This is expected since the selections

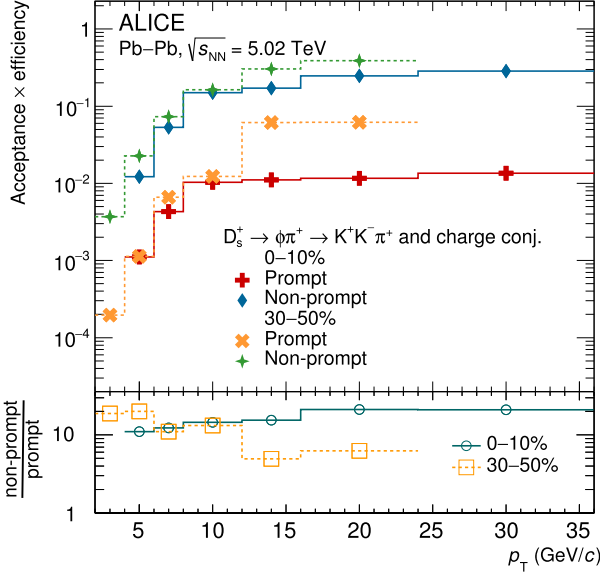


Fig. 2. Acceptance-times-efficiency factors for prompt and non-prompt D_s^+ mesons as a function of p_T in the 0–10% and 30–50% centrality intervals, together with their ratios (bottom panel).

applied to obtain the non-prompt enriched sample strongly suppress the prompt D_s^+ -meson efficiency. Instead, the acceptance is the same for prompt and non-prompt mesons. In central collisions, the prompt D_s^+ -meson suppression increases with increasing p_T . The opposite trend is observed in semicentral collisions, since less stringent selections on the BDT outputs are necessary to extract the non-prompt D_s^+ -meson signal due to the lower yield.

The fraction $f_{\text{non-prompt}}$ of non-prompt D_s^+ mesons in the extracted raw yield was estimated with a data-driven procedure based on the construction of data samples with different abundances of prompt and non-prompt candidates. These samples were built by varying the selection on the BDT output related to the candidate probability to be a non-prompt D_s^+ meson. Starting from the values of raw yield and acceptance times efficiency of prompt and non-prompt D_s^+ mesons obtained for each sample, the corrected yield of prompt and non-prompt D_s^+ mesons and the $f_{\text{non-prompt}}$ fraction were calculated. This data-driven technique does not depend on theoretical calculations of heavy-quark production and interaction with the QGP constituents, and it is described in detail in Ref. [52]. The $f_{\text{non-prompt}}$ fractions obtained as a function of p_T in central and semicentral Pb–Pb collisions are reported in Fig. 3, together with their statistical and systematic uncertainties. The determination of the systematic uncertainty on the $f_{\text{non-prompt}}$ fraction is described in Section 3. The $f_{\text{non-prompt}}$ values vary between about 0.72 (0.56) and 0.82 (0.70) in the 0–10% (30–50%) centrality interval as a function of transverse momentum. The $f_{\text{non-prompt}}$ is observed to be on average lower in semicentral collision with respect to central collisions. This difference is expected as in the 30–50% centrality interval less stringent BDT selections were applied compared to 0–10% centrality interval.

The non-prompt D_s^+ -meson nuclear modification factor, R_{AA} , was computed according to Eq. (1). The measurement of the p_T -differential cross section of non-prompt D_s^+ mesons at midrapidity ($|y| < 0.5$) in pp collisions at $\sqrt{s} = 5.02$ TeV from Ref. [52], which covers the transverse-momentum interval $2 < p_T < 12$ GeV/c, was used as the reference for the R_{AA} computation. For $p_T > 12$ GeV/c, an extrapolated pp reference was obtained from FONLL calculations of the beauty-hadron cross section and by using PYTHIA 8 to describe the decay kinematics of beauty hadrons to D_s^+ mesons, for more details see Ref. [52]. The resulting predictions were then scaled to match the measured values at lower transverse momenta.

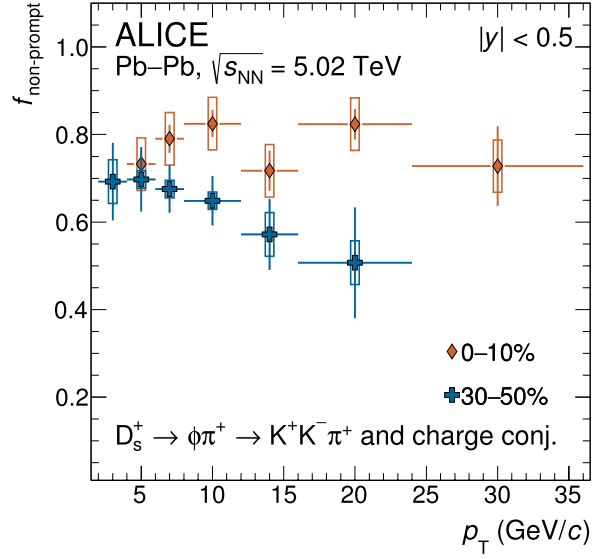


Fig. 3. Fraction of non-prompt D_s^+ mesons in the extracted raw yield as a function of p_T in the 0–10% and 30–50% centrality intervals. The vertical bars (boxes) report the statistical (systematic) uncertainties.

The total systematic uncertainty on the pp reference is $^{+38}_{-28}\%$ for all the extrapolated p_T intervals. The procedures for the p_T extrapolation and the systematic uncertainty estimation are the same as in Ref. [72].

3. Systematic uncertainties

The following sources of systematic uncertainty were considered for the production yield and R_{AA} estimation: (i) the raw-yield extraction, (ii) track reconstruction efficiency, (iii) non-prompt D_s^+ -meson fraction, (iv) BDT selection efficiency, (v) PID selection efficiency, (vi) relative abundances of beauty-hadron species in the MC simulation, and (vii) shapes of the simulated p_T -differential distributions. The resulting systematic uncertainties on the non-prompt D_s^+ -meson yield and R_{AA} in representative p_T intervals are summarised in Table 1. In the R_{AA} computation, the systematic uncertainties on the pp measurement were treated as uncorrelated from the ones on the Pb–Pb corrected yields, except for the uncertainty on the BR (3.6%) [51] which cancels in the R_{AA} and was considered only in the p_T -differential production yield. The normalisation uncertainty on the R_{AA} includes the uncertainty on the integrated luminosity in pp collisions (2.1% [73]), the uncertainty on the $\langle T_{\text{AA}} \rangle$ estimation, 0.7% (1.5%) for the 0–10% (30–50%) centrality interval [17], and the one related to the centrality-interval definition. This last contribution is due to the uncertainty on the fraction of the hadronic cross section used in the Glauber fit to determine the centrality. It was estimated to be < 0.1% and 2% for the 0–10% and 30–50% centrality intervals, respectively [72].

The systematic uncertainty on the raw-yield extraction was estimated by adopting several fit configurations changing the background fit function (linear and parabolic), the upper and lower fit limits, and the bin size of the invariant mass spectrum. The sensitivity to the line shape of the D_s^+ peak was tested by comparing the raw-yield values from the fits with those obtained by counting the candidates in the invariant mass region of the signal after subtracting the background estimated from the side bands.

The systematic uncertainty on the track reconstruction efficiency accounts for possible discrepancies between data and MC in the ITS–TPC prolongation efficiency and in the selection efficiency due to track-quality criteria in the TPC. The per-track systematic uncertainties were estimated by varying the track-quality selection criteria and by comparing the prolongation probability of the

Table 1

Systematic uncertainties on the measurement of the non-prompt D_s^+ -meson corrected yield and R_{AA} in the 0–10% and 30–50% centrality intervals for representative transverse-momentum intervals.

Centrality interval	0–10%		30–50%		
	p_T (GeV/c)	4–6	12–16	2–4	12–16
Yield extraction	5%	5%	10%	5%	
Tracking efficiency	13%	13%	11%	12%	
Non-prompt fraction	6%	6%	5%	6%	
Selection efficiency	8%	5%	10%	5%	
PID efficiency	negl.	negl.	negl.	negl.	
B hadrochemistry	1%	1%	1%	1%	
MC p_T shape	10%	8%	15%	2%	
Centrality limits		< 0.1%		2%	
$\langle T_{AA} \rangle$		0.7%		1.5%	
$\mathcal{L}_{\text{int}}^{\text{PP}}$			2.1%		
Branching ratio			3.6%		

TPC tracks to the ITS hits in data and simulations. They were then propagated to the non-prompt D_s^+ mesons via their decay kinematics.

The systematic uncertainties on the non-prompt D_s^+ -meson fraction and the BDT selection efficiency are due to possible discrepancies between data and MC in the distributions of the variables used in the BDT-model training (i.e. the D_s^+ -meson decay-vertex topology, kinematic, and PID variables). The former was computed by varying the configuration and the number of BDT selections employed in the data-driven method described in Sec. 2. In particular, wider and narrower intervals of the probability to be non-prompt D_s^+ mesons, and smaller and larger step sizes between the chosen BDT selections were considered. For each configuration, the non-prompt D_s^+ -meson fraction was recomputed. The systematic uncertainty related to the BDT selection efficiency was studied by repeating the entire analysis varying the selection criteria based on the BDT outputs. The uncertainty for this source of systematic uncertainty was assigned considering the RMS and the shift of the corrected yield obtained by varying the BDT selection with respect to the reference one.

Analogously, the systematic uncertainty on the PID selection efficiency relative to the loose selection on the PID variables applied before the BDT ones was also considered. This source was evaluated in the prompt D_s^+ -meson analysis [19], and it was found to be negligible for the adopted PID strategy.

The selection efficiency of non-prompt D_s^+ mesons originating from the decay of different beauty-hadron species can differ because of the different lifetime of the parent hadron and the different decay kinematics. Consequently, an imperfect description in the MC simulation of the beauty-hadron composition might result in a bias in the estimation of the D-meson efficiencies. This is especially important for D_s^+ mesons, which receive significant contributions from all the three ground-state B-meson species (B^+ , B^0 , and B_s^0). The PYTHIA 8 event generator describes the measurements of different B-meson species in pp collisions [52], however in heavy-ion collisions an enhanced production of strange over non-strange B mesons is expected compared to the one observed in pp collisions. Nevertheless, since no precise measurement of B_s^0 -meson production down to low momentum is available in Pb–Pb collisions, the relative abundances present in PYTHIA 8 were used without applying any reweighting. The systematic uncertainty introduced by this assumption was estimated by reweighting the B_s^0 contribution present in the MC enhanced by a factor 2 as predicted by the TAMU model [70]. The systematic uncertainty was assigned considering the variation between the production yield estimated using the enhanced B_s^0 contribution and the default one.

The systematic uncertainty due to the shape of the p_T distributions of D_s^+ mesons and beauty hadrons in the MC simulations was

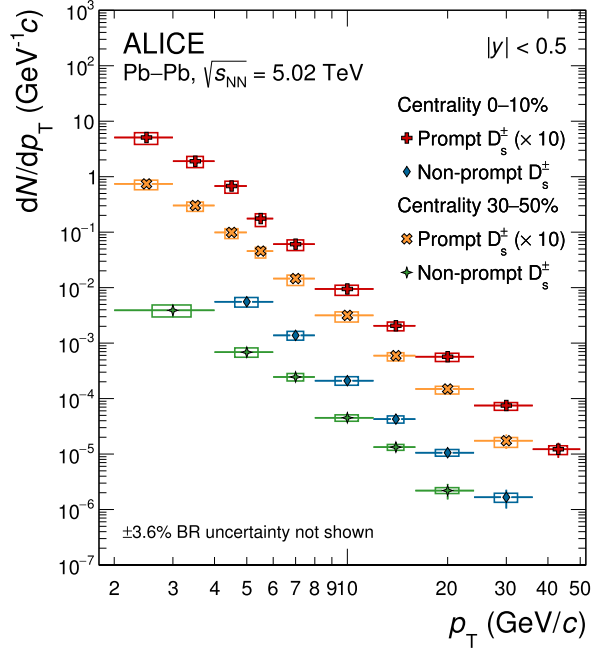


Fig. 4. Prompt and non-prompt D_s^+ meson production yield in central and semicentral Pb–Pb collisions at $\sqrt{s_{\text{NN}}} = 5.02$ TeV. The prompt D_s^+ results are taken from Ref. [19] and scaled by a factor 10 for visibility. The vertical bars (boxes) report the statistical (systematic) uncertainties.

evaluated by applying different weights to the p_T distributions of prompt D_s^+ mesons and of beauty-hadron mother particles in case of non-prompt D_s^+ mesons. As an alternative to the TAMU model, the shape resulting from the LIDO model [74] was considered. The main difference between the TAMU and LIDO model derives from the fact that the former includes the enhanced production of the B_s^0 mesons, unlike the latter. An additional variation of the shape of the p_T distributions of prompt D_s^+ mesons was included considering the results from Ref. [19]. The systematic uncertainty was assigned considering the variation of the corrected yield compared to the default case.

4. Results

Fig. 4 shows the p_T -differential production yield of prompt and non-prompt D_s^+ mesons in central and semicentral Pb–Pb collisions at $\sqrt{s_{\text{NN}}} = 5.02$ TeV. The measured prompt D_s^+ -meson production yields were taken from Ref. [19] and scaled by a factor 10 for visibility.

Fig. 5 reports the ratios of the production yield of non-prompt to prompt D_s^+ (left panel) and non-prompt D_s^+ to non-prompt D^0 [21] (right panel) in central and semicentral Pb–Pb collisions, as well as in pp collisions [52]. Computing these ratios helps to further investigate the effects of the QGP medium on the hadron formation mechanism. To get an indication of the B_s^0 -meson p_T probed by non-prompt D_s^+ mesons, a simulation with PYTHIA 8 was performed. As an example, the mean p_T distribution of B_s^0 mesons decaying to D_s^+ mesons with $4 < p_T < 6$ GeV/c has a mean of about 8.8 GeV/c and an RMS of about 3.1 GeV/c. The non-prompt to prompt D_s^+ -meson ratio ranges between about 0.05 and 0.20 and increases with increasing p_T up to $p_T = 10$ GeV/c. At higher momentum the slope of the ratios seems to reduce, even though no firm conclusions can be drawn with the current uncertainties. On the other hand, the non-prompt D_s^+ to non-prompt D^0 ratio shows an almost flat trend around 0.2 in the p_T range of the measurement. The ratios computed in pp and semicentral Pb–Pb

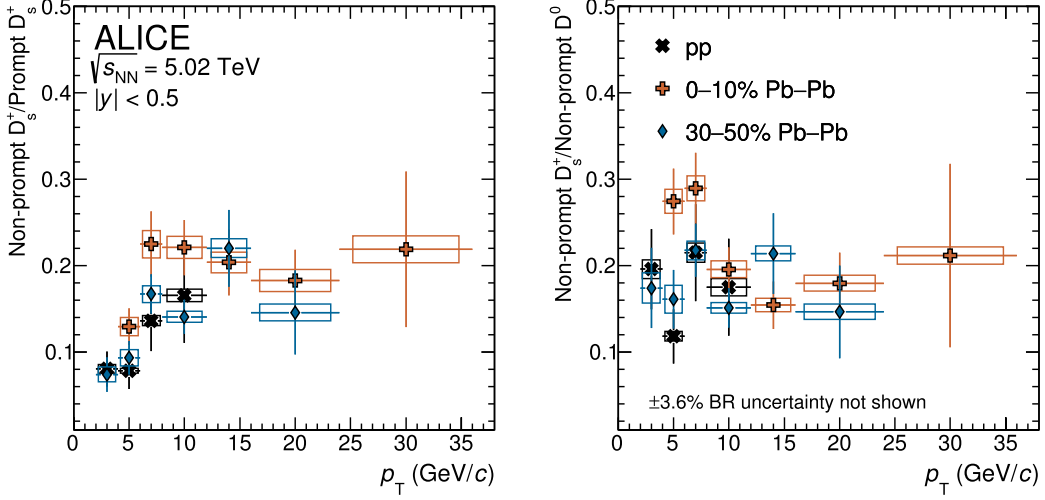


Fig. 5. The p_T -differential production yield of non-prompt D_s^+ mesons divided by those of prompt D_s^+ mesons (left panel) and non-prompt D^0 mesons (right panel) for the 0–10% and 30–50% centrality intervals in Pb–Pb collisions at $\sqrt{s_{NN}} = 5.02 \text{ TeV}$ from Refs. [19,21] compared with those in pp collisions at the same centre-of-mass energy from Ref. [52].

collisions are compatible within the uncertainties. A hint of enhancement compared to pp collisions with a significance of 1.7σ , where σ indicates the sum in quadrature of statistical and systematic uncertainties, is found by performing a weighted average of the non-prompt D_s^+/D^0 values in the $4 < p_T < 12 \text{ GeV}/c$ interval for the 0–10% centrality class. The inverse of the squared sum of the relative statistical and p_T -uncorrelated systematic uncertainties was used as weight in the average. All the systematic uncertainties, except for those on the raw-yield extraction, were considered as fully correlated in p_T . This hint of a larger non-prompt D_s^+/D^0 yield ratio is consistent with an enhanced production of strange-beauty mesons in heavy-ion collisions compared to pp collisions, as expected in a scenario in which beauty quarks hadronise via recombination with surrounding quarks in the strangeness-enriched QGP medium. In the transverse-momentum interval $4 < p_T < 12 \text{ GeV}/c$, also the non-prompt to prompt D_s^+ -meson ratio in the 0–10% centrality class shows a mild enhancement with respect to pp collisions with a significance of 1.6σ .

The R_{AA} of non-prompt D_s^+ mesons was computed according to Eq. (1), where the pp reference was obtained from the measurement published in Ref. [52]. To study the effects of the QGP medium on the resulting momentum spectra and the hadronisation mechanism of beauty quarks, the nuclear modification factor measured for the non-prompt D_s^+ mesons was compared to that of prompt D_s^+ [19] and non-prompt D^0 [21] mesons measured at the same centre-of-mass energy per nucleon pair. The prompt and non-prompt D_s^+ R_{AA} are compared in the top- and bottom-left panels of Fig. 6 for the 0–10% and 30–50% centrality class, respectively. Analogously, the comparison between the nuclear modification factor of non-prompt D_s^+ and non-prompt D^0 mesons is reported in the right panels of the same figure. The R_{AA} of prompt and non-prompt D mesons shows a decreasing trend with increasing p_T up to a minimum of about 0.2 (0.4) around $10 \text{ GeV}/c$ in the 0–10% (30–50%) centrality class. In the lowest p_T intervals, the R_{AA} increases up to unity. In particular, the central values of the non-prompt D_s^+ R_{AA} are higher with respect to those of prompt D_s^+ and non-prompt D^0 in the 0–10% centrality class for $p_T < 6 \text{ GeV}/c$, even though they are compatible within uncertainties. This possible difference between prompt and non-prompt D_s^+ R_{AA} would be consistent with the different loss of energy experienced by charm and beauty quarks traversing the QGP. In fact, the effect due to the different decay kinematics of charm and beauty hadrons is found to be negligible, as discussed in Ref. [21]. Instead,

the difference between non-prompt D_s^+ and D^0 mesons could result from the hadronisation via recombination and the presence of a strangeness-rich environment. In semicentral collisions, no separation among the R_{AA} of prompt D_s^+ , non-prompt D_s^+ , and non-prompt D^0 is observed within the measurement uncertainties.

The R_{AA} measurements were compared with the predictions of the TAMU model [70]. In the TAMU model, the heavy-quark transport is described via the Langevin equation and the hadronisation can occur both via recombination with light quarks from the medium, which is the dominant mechanism at low p_T , or via fragmentation, which becomes more important at high p_T . The TAMU predictions are shown in Fig. 6. The uncertainty band for prompt D_s^+ mesons is due to the modification of the parton distribution functions in Pb nuclei, which is neglected for the beauty-quark production. The TAMU model qualitatively describes the p_T trend of the non-prompt D_s^+ -meson R_{AA} , although it overestimates the measurements.

In the left and right panels of Fig. 7, the nuclear modification factors of non-prompt D_s^+ mesons divided by that of prompt D_s^+ mesons and non-prompt D^0 mesons are shown, respectively. The measurements in both centrality intervals are compared with the predictions of the TAMU model. In the 0–10% centrality class, the non-prompt D_s^+ to prompt D_s^+ R_{AA} ratio suggests a hint of enhancement with a statistical significance of 1.6σ in the $4 < p_T < 12 \text{ GeV}/c$ interval, which is by construction the same of that reported for the corresponding yield ratio. The R_{AA} ratio is consistent with a larger energy loss for the charm quark with respect to the beauty quark due to its smaller mass, as already suggested by the results shown in Fig. 6. No hint for a ratio of the R_{AA} larger than unity is observed in semicentral collisions. Considering the measurement uncertainties, TAMU predictions qualitatively describe the results for central collisions. At variance, for semicentral collisions the TAMU model overestimates the R_{AA} ratio values. The measurements of the non-prompt D_s^+ to non-prompt D^0 R_{AA} ratio suggest a possible enhancement with respect to unity in the $4 < p_T < 12 \text{ GeV}/c$ interval for central collisions, as reported for the yield ratio. In this case, the rise at low p_T might be a consequence of the abundance of strange quarks thermally produced in the QGP and the dominance of the hadronisation via recombination in this range of momentum. The TAMU model describes the data within the experimental uncertainties.

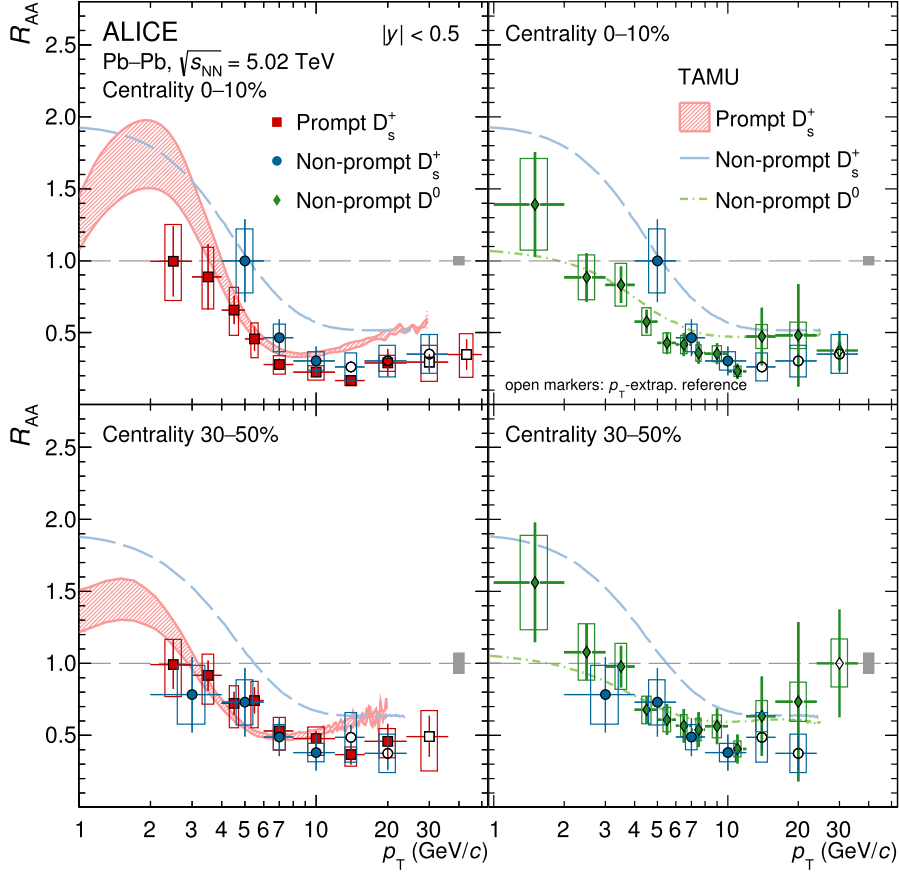


Fig. 6. Left panels: prompt (Ref. [19]) and non-prompt D_s^+ -meson R_{AA} in central (top) and semicentral (bottom) Pb-Pb collisions at $\sqrt{s_{NN}} = 5.02$ TeV. Right panels: non-prompt D_s^+ - and D^0 -meson (Ref. [21]) R_{AA} in central (top) and semicentral (bottom) Pb-Pb collisions at $\sqrt{s_{NN}} = 5.02$ TeV. The experimental results are compared with the predictions of the TAMU model [70]. Statistical (bars), systematic (boxes), and normalisation (shaded box around unity) uncertainties are shown.

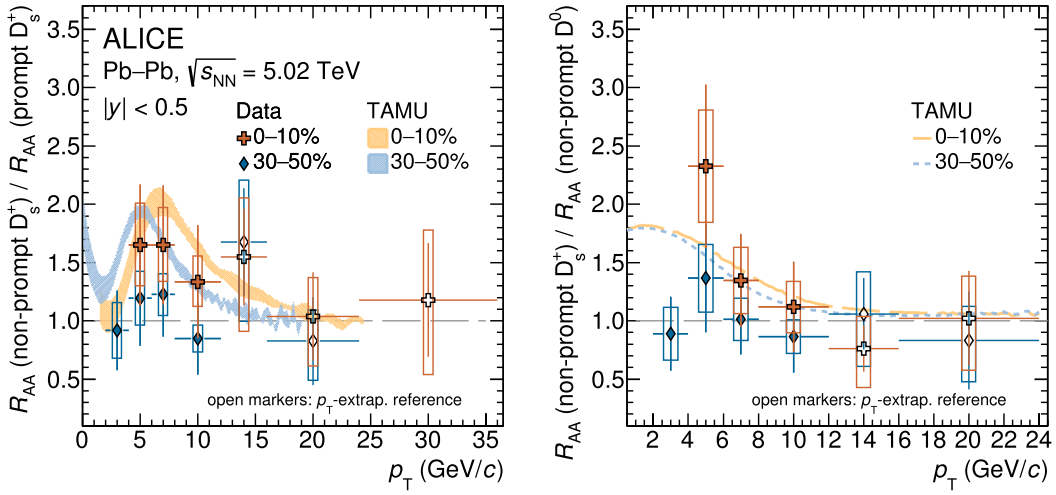


Fig. 7. The R_{AA} of non-prompt D_s^+ mesons divided by the one of prompt D_s^+ mesons [19] (left panel) and non-prompt D^0 mesons [21] (right panel) for the 0-10% and 30-50% centrality intervals in Pb-Pb collisions at $\sqrt{s_{NN}} = 5.02$ TeV. The measurements are compared with TAMU model predictions [70]. Statistical (bars) and systematic (boxes) uncertainties are shown.

5. Conclusions

In this Letter, the first measurement of the non-prompt D_s^+ -meson production at midrapidity in Pb-Pb collisions at $\sqrt{s_{NN}} = 5.02$ TeV was reported.

The non-prompt D_s^+ -meson production yield was measured between 4 and 36 (2 and 24) GeV/c in the 0-10% (30-50%) centrality interval. These measurements were compared to the ones

performed for prompt D_s^+ and non-prompt D^0 mesons at the same centre-of-mass energy. The production yield was employed to compute the non-prompt D_s^+ -meson R_{AA} , which was compared with the R_{AA} of prompt D_s^+ and non-prompt D^0 mesons.

The non-prompt D_s^+ R_{AA} shows a significant p_T dependence. A minimum at intermediate transverse momentum ($p_T \approx 10 \text{ GeV}/c$) around 0.2 (0.4) in central (semicentral) collisions, and a mild increase with decreasing p_T , with R_{AA} reaching (close to) unity at

$p_T \approx 4\text{--}6$ (2–4) GeV/c in the 0–10% (30–50%) centrality interval are reported. The TAMU model, which implements the parton in-medium energy loss through collisional processes as well as the beauty-quark hadronisation both via fragmentation and recombination, describes the p_T trend of the R_{AA} . However, it overestimates the measurements. Further comparisons were performed between prompt and non-prompt D_s^+ as well as non-prompt D^0 mesons by computing the ratios of their production yields and R_{AA} . These ratios suggest the presence of an enhancement of non-prompt D_s^+ mesons compared to prompt D_s^+ (non-prompt D^0) mesons in central collisions in the $4 < p_T < 12$ GeV/c interval, with a significance of 1.6σ (1.7σ). The increase is consistent with expectations for the overall effect of the energy-loss mechanism and the hadronisation-process modification in presence of the colour-deconfined medium.

The recent upgrade of the ALICE apparatus will greatly enhance the physics potential of the experiment in the LHC Run 3 data-taking period, allowing for more precise measurements of the non-prompt D_s^+ -meson production in heavy-ion collisions.

Declaration of competing interest

The authors declare that they have no known competing financial interests or personal relationships that could have appeared to influence the work reported in this paper.

Data availability

This manuscript has associated data in a HEPData repository at: <https://www.hepdata.net/record/ins2071181>.

Acknowledgements

The ALICE Collaboration would like to thank all its engineers and technicians for their invaluable contributions to the construction of the experiment and the CERN accelerator teams for the outstanding performance of the LHC complex. The ALICE Collaboration gratefully acknowledges the resources and support provided by all Grid centres and the Worldwide LHC Computing Grid (WLCG) collaboration. The ALICE Collaboration acknowledges the following funding agencies for their support in building and running the ALICE detector: A. I. Alikhanyan National Science Laboratory (Yerevan Physics Institute) Foundation (ANSL), State Committee of Science and World Federation of Scientists (WFS), Armenia; Austrian Academy of Sciences, Austrian Science Fund (FWF): [M 2467-N36] and Nationalstiftung für Forschung, Technologie und Entwicklung, Austria; Ministry of Communications and High Technologies, National Nuclear Research Center, Azerbaijan; Conselho Nacional de Desenvolvimento Científico e Tecnológico (CNPq), Fincantieri de Estudos e Projetos (Finep), Fundação de Amparo à Pesquisa do Estado de São Paulo (FAPESP) and Universidade Federal do Rio Grande do Sul (UFRGS), Brazil; Bulgarian Ministry of Education and Science, within the National Roadmap for Research Infrastructures 2020–2027 (object CERN), Bulgaria; Ministry of Education of China (MOEC), Ministry of Science & Technology of China (MSTC) and National Natural Science Foundation of China (NSFC), China; Ministry of Science and Education and Croatian Science Foundation, Croatia; Centro de Aplicaciones Tecnológicas y Desarrollo Nuclear (CEADEN), Cubaenergía, Cuba; The Ministry of Education, Youth and Sports of the Czech Republic, Czech Republic; The Danish Council for Independent Research | Natural Sciences, the Villum Fonden and Danish National Research Foundation (DNRF), Denmark; Helsinki Institute of Physics (HIP), Finland; Commissariat à l’Energie Atomique (CEA) and Institut National de Physique Nucléaire et de Physique des Particules (IN2P3) and Centre National de la Recherche Scientifique (CNRS), France; Bundesminis-

terium für Bildung und Forschung (BMBF) and GSI Helmholtzzentrum für Schwerionenforschung GmbH, Germany; General Secretariat for Research and Technology, Ministry of Education, Research and Religions, Greece; National Research, Development and Innovation Office, Hungary; Department of Atomic Energy Government of India (DAE), Department of Science and Technology, Government of India (DST), University Grants Commission, Government of India (UGC) and Council of Scientific and Industrial Research (CSIR), India; National Research and Innovation Agency - BRIN, Indonesia; Istituto Nazionale di Fisica Nucleare (INFN), Italy; Japanese Ministry of Education, Culture, Sports, Science and Technology (MEXT) and Japan Society for the Promotion of Science (JSPS) KAKENHI, Japan; Consejo Nacional de Ciencia y Tecnología (CONACYT), through Fondo de Cooperación Internacional en Ciencia y Tecnología (FONCICYT) and Dirección General de Asuntos del Personal Académico (DGAPA), Mexico; Nederlandse Organisatie voor Wetenschappelijk Onderzoek (NWO), Netherlands; The Research Council of Norway, Norway; Commission on Science and Technology for Sustainable Development in the South (COMSATS), Pakistan; Pontificia Universidad Católica del Perú, Peru; Ministry of Education and Science, National Science Centre and WUT ID-UB, Poland; Korea Institute of Science and Technology Information and National Research Foundation of Korea (NRF), Republic of Korea; Ministry of Education and Scientific Research, Institute of Atomic Physics, Ministry of Research and Innovation and Institute of Atomic Physics and University Politehnica of Bucharest, Romania; Ministry of Education, Science, Research and Sport of the Slovak Republic, Slovakia; National Research Foundation of South Africa, South Africa; Swedish Research Council (VR) and Knut & Alice Wallenberg Foundation (KAW), Sweden; European Organization for Nuclear Research, Switzerland; Suranaree University of Technology (SUT), National Science and Technology Development Agency (NSTDA) and National Science, Research and Innovation Fund (NSRF via PMU-B B05F650021), Thailand; Turkish Energy, Nuclear and Mineral Research Agency (TENMAK), Turkey; National Academy of Sciences of Ukraine, Ukraine; Science and Technology Facilities Council (STFC), United Kingdom; National Science Foundation of the United States of America (NSF) and United States Department of Energy, Office of Nuclear Physics (DOE NP), United States of America. In addition, individual groups or members have received support from: Marie Skłodowska Curie, Strong 2020 – Horizon 2020, European Research Council (grant nos. 824093, 896850, 950692), European Union; Academy of Finland (Center of Excellence in Quark Matter) (grant nos. 346327, 346328), Finland; Programa de Apoyos para la Superación del Personal Académico, UNAM, Mexico.

References

- [1] F. Karsch, Lattice simulations of the thermodynamics of strongly interacting elementary particles and the exploration of new phases of matter in relativistic heavy ion collisions, *J. Phys. Conf. Ser.* 46 (2006) 122–131, arXiv: hep-lat/0608003.
- [2] S. Borsanyi, Z. Fodor, J.N. Guenther, R. Kara, S.D. Katz, P. Parotto, A. Pasztor, C. Ratti, K.K. Szabo, QCD crossover at finite chemical potential from lattice simulations, *Phys. Rev. Lett.* 125 (5) (2020) 052001, arXiv:2002.02821 [hep-lat].
- [3] HotQCD Collaboration, A. Bazavov, et al., Chiral crossover in QCD at zero and non-zero chemical potentials, *Phys. Lett. B* 795 (2019) 15–21, arXiv:1812.08235 [hep-lat].
- [4] U.W. Heinz, M. Jacob, Evidence for a new state of matter: an assessment of the results from the CERN lead beam program, arXiv:nucl-th/0002042.
- [5] BRAHMS Collaboration, I. Arsene, et al., Quark gluon plasma and color glass condensate at RHIC? The perspective from the BRAHMS experiment, *Nucl. Phys. A* 757 (2005) 1–27, arXiv:nucl-ex/0410020.
- [6] PHOBOS Collaboration, B.B. Back, et al., The PHOBOS perspective on discoveries at RHIC, *Nucl. Phys. A* 757 (2005) 28–101, arXiv:nucl-ex/0410022.
- [7] STAR Collaboration, J. Adams, et al., Experimental and theoretical challenges in the search for the quark gluon plasma: the STAR Collaboration’s critical assessment of the evidence from RHIC collisions, *Nucl. Phys. A* 757 (2005) 102–183, arXiv:nucl-ex/0501009.

- [8] PHENIX Collaboration, K. Adcox, et al., Formation of dense partonic matter in relativistic nucleus-nucleus collisions at RHIC: experimental evaluation by the PHENIX collaboration, *Nucl. Phys. A* 757 (2005) 184–283, arXiv:nucl-ex/0410003.
- [9] ALICE Collaboration, S. Acharya, et al., Transverse momentum spectra and nuclear modification factors of charged particles in pp, p-Pb and Pb-Pb collisions at the LHC, *J. High Energy Phys.* 11 (2018) 013, arXiv:1802.09145 [nucl-ex].
- [10] ALICE Collaboration, J. Adam, et al., Anisotropic flow of charged particles in Pb-Pb collisions at $\sqrt{s_{NN}} = 5.02$ TeV, *Phys. Rev. Lett.* 116 (13) (2016) 132302, arXiv:1602.01119 [nucl-ex].
- [11] P. Braun-Munzinger, V. Koch, T. Schäfer, J. Stachel, Properties of hot and dense matter from relativistic heavy ion collisions, *Phys. Rep.* 621 (2016) 76–126, arXiv:1510.00442 [nucl-th].
- [12] M.H. Thoma, M. Gyulassy, Quark damping and energy loss in the high temperature QCD, *Nucl. Phys. B* 351 (1991) 491–506.
- [13] E. Braaten, M.H. Thoma, Energy loss of a heavy fermion in a hot plasma, *Phys. Rev. D* 44 (1991) 1298–1310.
- [14] E. Braaten, M.H. Thoma, Energy loss of a heavy quark in the quark - gluon plasma, *Phys. Rev. D* 44 (9) (1991) R2625.
- [15] R. Baier, Y.L. Dokshitzer, A.H. Mueller, S. Peigné, D. Schiff, Radiative energy loss and p_T broadening of high-energy partons in nuclei, *Nucl. Phys. B* 484 (1997) 265–282, arXiv:hep-ph/9608322.
- [16] M. Gyulassy, M. Plumer, Jet quenching in dense matter, *Phys. Lett. B* 243 (1990) 432–438.
- [17] ALICE Collaboration, Centrality determination in heavy ion collisions, ALICE-PUBLIC-2018-011, <https://cds.cern.ch/record/2636623>, Aug 2018.
- [18] ALICE Collaboration, S. Acharya, et al., Prompt D^0 , D^+ , and D^{*+} production in Pb-Pb collisions at $\sqrt{s_{NN}} = 5.02$ TeV, *J. High Energy Phys.* 01 (2022) 174, arXiv:2110.09420 [nucl-ex].
- [19] ALICE Collaboration, S. Acharya, et al., Measurement of prompt D_s^{*+} -meson production and azimuthal anisotropy in Pb-Pb collisions at $\sqrt{s_{NN}} = 5.02$ TeV, *Phys. Lett. B* 827 (2022) 136986, arXiv:2110.10006 [nucl-ex].
- [20] ALICE Collaboration, S. Acharya, et al., Constraining hadronization mechanisms with Λ_c^+/D^0 production ratios in Pb-Pb collisions at $\sqrt{s_{NN}} = 5.02$ TeV, arXiv: 2112.08156 [nucl-ex].
- [21] ALICE Collaboration, S. Acharya, et al., Measurement of beauty production via non-prompt D^0 mesons in Pb-Pb collisions at $\sqrt{s_{NN}} = 5.02$ TeV, arXiv:2202.00815 [nucl-ex].
- [22] CMS Collaboration, A.M. Sirunyan, et al., Nuclear modification factor of D^0 mesons in PbPb collisions at $\sqrt{s_{NN}} = 5.02$ TeV, *Phys. Lett. B* 782 (2018) 474–496, arXiv:1708.04962 [nucl-ex].
- [23] CMS Collaboration, A.M. Sirunyan, et al., Measurement of the B^\pm meson nuclear modification factor in Pb-Pb collisions at $\sqrt{s_{NN}} = 5.02$ TeV, *Phys. Rev. Lett.* 119 (15) (2017) 152301, arXiv:1705.04727 [hep-ex].
- [24] CMS Collaboration, A.M. Sirunyan, et al., Measurement of prompt and non-prompt charmonium suppression in PbPb collisions at 5.02 TeV, *Eur. Phys. J. C* 78 (6) (2018) 509, arXiv:1712.08959 [nucl-ex].
- [25] CMS Collaboration, A.M. Sirunyan, et al., Studies of beauty suppression via non-prompt D^0 mesons in Pb-Pb collisions at $\sqrt{s_{NN}} = 5.02$ TeV, *Phys. Rev. Lett.* 123 (2) (2019) 022001, arXiv:1810.11102 [hep-ex].
- [26] CMS Collaboration, A.M. Sirunyan, et al., Measurement of B_s^0 meson production in pp and PbPb collisions at $\sqrt{s_{NN}} = 5.02$ TeV, *Phys. Lett. B* 796 (2019) 168–190, arXiv:1810.03022 [hep-ex].
- [27] CMS Collaboration, A.M. Sirunyan, et al., Production of Λ_c^+ baryons in proton-proton and lead-lead collisions at $\sqrt{s_{NN}} = 5.02$ TeV, *Phys. Lett. B* 803 (2020) 135328, arXiv:1906.03322 [hep-ex].
- [28] ALICE Collaboration, J. Adam, et al., Measurement of electrons from beauty-hadron decays in p-Pb collisions at $\sqrt{s_{NN}} = 5.02$ TeV and Pb-Pb collisions at $\sqrt{s_{NN}} = 2.76$ TeV, *J. High Energy Phys.* 07 (2017) 052, arXiv:1609.03898 [nucl-ex].
- [29] ATLAS Collaboration, M. Aaboud, et al., Prompt and non-prompt J/ψ and $\psi(2S)$ suppression at high transverse momentum in 5.02 TeV Pb+Pb collisions with the ATLAS experiment, *Eur. Phys. J. C* 78 (9) (2018) 762, arXiv:1805.04077 [nucl-ex].
- [30] ATLAS Collaboration, G. Aad, et al., Measurement of the nuclear modification factor for muons from charm and bottom hadrons in Pb+Pb collisions at 5.02 TeV with the ATLAS detector, *Phys. Lett. B* 829 (2022) 137077, arXiv: 2109.00411 [nucl-ex].
- [31] STAR Collaboration, J. Adam, et al., Centrality and transverse momentum dependence of D^0 -meson production at mid-rapidity in Au+Au collisions at $\sqrt{s_{NN}} = 200$ GeV, *Phys. Rev. C* 99 (3) (2019) 034908, arXiv:1812.10224 [nucl-ex].
- [32] STAR Collaboration, S. Collaboration, et al., Evidence of mass ordering of charm and bottom quark energy loss in Au+Au collisions at RHIC, arXiv:2111.14615 [nucl-ex].
- [33] PHENIX Collaboration, A. Adare, et al., Single electron yields from semileptonic charm and bottom hadron decays in Au+Au collisions at $\sqrt{s_{NN}} = 200$ GeV, *Phys. Rev. C* 93 (3) (2016) 034904, arXiv:1509.04662 [nucl-ex].
- [34] Y.L. Dokshitzer, V.A. Khoze, S.I. Troian, On specific QCD properties of heavy quark fragmentation ('dead cone'), *J. Phys. G* 17 (1991) 1602–1604.
- [35] ALICE Collaboration, S. Acharya, et al., Direct observation of the dead-cone effect in QCD, arXiv:2106.05713 [nucl-ex].
- [36] B. Svetitsky, Diffusion of charmed quarks in the quark-gluon plasma, *Phys. Rev. D* 37 (1988) 2484–2491.
- [37] ALICE Collaboration, S. Acharya, et al., Transverse-momentum and event-shape dependence of D-meson flow harmonics in Pb-Pb collisions at $\sqrt{s_{NN}} = 5.02$ TeV, *Phys. Lett. B* 813 (2021) 136054, arXiv:2005.11131 [nucl-ex].
- [38] A. Beraudo, et al., Extraction of heavy-flavor transport coefficients in QCD matter, *Nucl. Phys. A* 979 (2018) 21–86, arXiv:1803.03824 [nucl-th].
- [39] J. Rafelski, B. Müller, Strangeness production in the quark - gluon plasma, *Phys. Rev. Lett.* 48 (1982) 1066, Erratum: *Phys. Rev. Lett.* 56 (1986) 2334.
- [40] P. Koch, B. Müller, J. Rafelski, Strangeness in relativistic heavy ion collisions, *Phys. Rep.* 142 (1986) 167–262.
- [41] STAR Collaboration, J. Adam, et al., Observation of D_s^\pm/D^0 enhancement in Au+Au collisions at $\sqrt{s_{NN}} = 200$ GeV, *Phys. Rev. Lett.* 127 (2021) 092301, arXiv:2101.11793 [hep-ex].
- [42] ALICE Collaboration, S. Acharya, et al., Measurement of D^0 , D^+ , D^{*+} and D_s^+ production in Pb-Pb collisions at $\sqrt{s_{NN}} = 5.02$ TeV, *J. High Energy Phys.* 10 (2018) 174, arXiv:1804.09083 [nucl-ex].
- [43] CMS Collaboration, A. Tumasyan, et al., Observation of $Bs0$ mesons and measurement of the $Bs0/B^+$ yield ratio in PbPb collisions at Image 1 TeV, *Phys. Lett. B* 829 (2022) 137062, arXiv:2109.01908 [hep-ex].
- [44] STAR Collaboration, J. Adam, et al., First measurement of Λ_c baryon production in Au+Au collisions at $\sqrt{s_{NN}} = 200$ GeV, *Phys. Rev. Lett.* 124 (17) (2020) 172301, arXiv:1910.14628 [nucl-ex].
- [45] ALICE Collaboration, J. Adam, et al., J/ψ suppression at forward rapidity in Pb-Pb collisions at $\sqrt{s_{NN}} = 5.02$ TeV, *Phys. Lett. B* 766 (2017) 212–224, arXiv: 1606.08197 [nucl-ex].
- [46] ALICE Collaboration, S. Acharya, et al., Studies of J/ψ production at forward rapidity in Pb-Pb collisions at $\sqrt{s_{NN}} = 5.02$ TeV, *J. High Energy Phys.* 02 (2020) 041, arXiv:1909.03158 [nucl-ex].
- [47] ALICE Collaboration, S. Acharya, et al., Centrality and transverse momentum dependence of inclusive J/ψ production at midrapidity in Pb-Pb collisions at $\sqrt{s_{NN}} = 5.02$ TeV, *Phys. Lett. B* 805 (2020) 135434, arXiv:1910.14404 [nucl-ex].
- [48] ALICE Collaboration, S. Acharya, et al., Observation of a multiplicity dependence in the p_T -differential charm baryon-to-meson ratios in proton-proton collisions at $\sqrt{s} = 13$ TeV, *Phys. Lett. B* 829 (2022) 137065, arXiv:2111.11948 [nucl-ex].
- [49] LHCb Collaboration, Evidence for modification of b quark hadronization in high-multiplicity pp collisions at $\sqrt{s} = 13$ TeV, arXiv:2204.13042 [hep-ex].
- [50] ALICE Collaboration, J. Adam, et al., Enhanced production of multi-strange hadrons in high-multiplicity proton-proton collisions, *Nat. Phys.* 13 (2017) 535–539, arXiv:1606.07424 [nucl-ex].
- [51] Particle Data Group Collaboration, P. Zyla, et al., Review of particle physics, *PTEP* 2020 (8) (2020), 083C01.
- [52] ALICE Collaboration, S. Acharya, et al., Measurement of beauty and charm production in pp collisions at $\sqrt{s} = 5.02$ TeV via non-prompt and prompt D mesons, *J. High Energy Phys.* 05 (2021) 220, arXiv:2102.13601 [nucl-ex].
- [53] ALICE Collaboration, K. Aamodt, et al., Alignment of the ALICE Inner Tracking System with cosmic-ray tracks, *J. Instrum.* 5 (2010) P03003, arXiv:1001.0502 [physics.ins-det].
- [54] J. Alme, et al., The ALICE TPC, a large 3-dimensional tracking device with fast readout for ultra-high multiplicity events, *Nucl. Instrum. Methods A* 622 (2010) 316–367, arXiv:1001.1950 [physics.ins-det].
- [55] A. Akindinov, et al., Performance of the ALICE Time-Of-Flight detector at the LHC, *Eur. Phys. J. Plus* 128 (2013) 44.
- [56] ALICE Collaboration, E. Abbas, et al., Performance of the ALICE VZERO system, *J. Instrum.* 8 (2013) P10016, arXiv:1306.3130 [nucl-ex].
- [57] ALICE Collaboration, B. Abelev, et al., Performance of the ALICE experiment at the CERN LHC, *Int. J. Mod. Phys. A* 29 (2014) 1430044, arXiv:1402.4476 [nucl-ex].
- [58] ALICE Collaboration, J. Adam, et al., Centrality dependence of the charged-particle multiplicity density at midrapidity in Pb-Pb collisions at $\sqrt{s_{NN}} = 5.02$ TeV, *Phys. Rev. Lett.* 116 (22) (2016) 222302, arXiv:1512.06104 [nucl-ex].
- [59] C. Loizides, J. Kamín, D. d'Enterria, Improved Monte Carlo Glauber predictions at present and future nuclear colliders, *Phys. Rev. C* 97 (5) (2018) 054910, arXiv:1710.07098 [nucl-ex], Erratum: *Phys. Rev. C* 99 (2019) 019901.
- [60] D. d'Enterria, C. Loizides, Progress in the Glauber model at collider energies, *Annu. Rev. Nucl. Part. Sci.* 71 (2021) 315–344, arXiv:2011.14909 [hep-ph].
- [61] T. Chen, C. Guestrin, Xgboost: a scalable tree boosting system, in: *Proceedings of the 22nd ACM SIGKDD International Conference on Knowledge Discovery and Data Mining*, 2016, pp. 785–794, arXiv:1603.02754 [cs.LG].
- [62] L. Barioglio, F. Catalano, M. Concas, P. Feccio, F. Grossa, F. Mazzaschi, M. Puccio, hipe4ml/hipe4ml, <https://doi.org/10.5281/zenodo.5070132>, July, 2021.
- [63] X.-N. Wang, M. Gyulassy, Hijing: a Monte Carlo model for multiple jet production in pp, pA, and AA collisions, *Phys. Rev. D* 44 (Dec 1991) 3501–3516.
- [64] T. Sjostrand, S. Mrenna, P.Z. Skands, PYTHIA 6.4 physics and manual, *J. High Energy Phys.* 05 (2006) 026, arXiv:hep-ph/0603175.
- [65] T. Sjöstrand, S. Ask, J.R. Christiansen, R. Corke, N. Desai, P. Ilten, S. Mrenna, S. Prestel, C.O. Rasmussen, P.Z. Skands, An introduction to PYTHIA 8.2, *Comput. Phys. Commun.* 191 (2015) 159–177, arXiv:1410.3012 [hep-ph].

- [66] P. Skands, S. Carrazza, J. Rojo, Tuning PYTHIA 8.1: the Monash 2013 Tune, *Eur. Phys. J. C* **74** (8) (2014) 3024, arXiv:1404.5630 [hep-ph].
- [67] R. Brun, F. Bruylants, F. Carminati, S. Giani, M. Maire, A. McPherson, G. Patrick, L. Urban, GEANT: Detector Description and Simulation Tool; Oct 1994, CERN Program Library, CERN, Geneva, Oct 1994, <http://cds.cern.ch/record/1082634>, 1993, Long Writeup W5013.
- [68] M. Cacciari, M. Greco, P. Nason, The p_T spectrum in heavy-flavor hadroproduction, *J. High Energy Phys.* **05** (1998) 007, arXiv:hep-ph/9803400 [hep-ph].
- [69] M. Cacciari, S. Frixione, P. Nason, The p_T spectrum in heavy-flavor photoproduction, *J. High Energy Phys.* **03** (2001) 006, arXiv:hep-ph/0102134 [hep-ph].
- [70] M. He, R.J. Fries, R. Rapp, Heavy flavor at the large hadron collider in a strong coupling approach, *Phys. Lett. B* **735** (2014) 445–450, arXiv:1401.3817 [nucl-th].
- [71] M. He, R. Rapp, Hadronization and charm-hadron ratios in heavy-ion collisions, *Phys. Rev. Lett.* **124** (4) (2020) 042301, arXiv:1905.09216 [nucl-th].
- [72] ALICE Collaboration, J. Adam, et al., Transverse momentum dependence of D-meson production in Pb-Pb collisions at $\sqrt{s_{NN}} = 2.76$ TeV, *J. High Energy Phys.* **03** (2016) 081, arXiv:1509.06888 [nucl-ex].
- [73] ALICE Collaboration, ALICE 2017 luminosity determination for pp collisions at $\sqrt{s} = 5$ TeV, ALICE-PUBLIC-2018-014, <http://cds.cern.ch/record/2648933>, Nov 2018.
- [74] W. Ke, Y. Xu, S.A. Bass, Linearized Boltzmann-Langevin model for heavy quark transport in hot and dense QCD matter, *Phys. Rev. C* **98** (6) (2018) 064901, arXiv:1806.08848 [nucl-th].

ALICE Collaboration

- S. Acharya ^{123,131, ID}, D. Adamová ^{85, ID}, A. Adler ⁶⁹, G. Aglieri Rinella ^{32, ID}, M. Agnello ^{29, ID}, N. Agrawal ^{50, ID}, Z. Ahammed ^{131, ID}, S. Ahmad ^{15, ID}, S.U. Ahn ^{70, ID}, I. Ahuja ^{37, ID}, A. Akindinov ^{139, ID}, M. Al-Turany ^{97, ID}, D. Aleksandrov ^{139, ID}, B. Alessandro ^{55, ID}, H.M. Alfanda ^{6, ID}, R. Alfaro Molina ^{66, ID}, B. Ali ^{15, ID}, Y. Ali ¹³, A. Alici ^{25, ID}, N. Alizadehvandchali ^{112, ID}, A. Alkin ^{32, ID}, J. Alme ^{20, ID}, G. Alococo ^{51, ID}, T. Alt ^{63, ID}, I. Altsybeev ^{139, ID}, M.N. Anaam ^{6, ID}, C. Andrei ^{45, ID}, A. Andronic ^{134, ID}, V. Anguelov ^{94, ID}, F. Antinori ^{53, ID}, P. Antonioli ^{50, ID}, C. Anuj ^{15, ID}, N. Apadula ^{73, ID}, L. Aphecetche ^{102, ID}, H. Appelshäuser ^{63, ID}, S. Arcelli ^{25, ID}, R. Arnaldi ^{55, ID}, I.C. Arsene ^{19, ID}, M. Arslanbekov ^{136, ID}, A. Augustinus ^{32, ID}, R. Averbeck ^{97, ID}, S. Aziz ^{127, ID}, M.D. Azmi ^{15, ID}, A. Badalà ^{52, ID}, Y.W. Baek ^{40, ID}, X. Bai ^{97, ID}, R. Bailhache ^{63, ID}, Y. Bailung ^{47, ID}, R. Bala ^{90, ID}, A. Balbino ^{29, ID}, A. Baldissari ^{126, ID}, B. Balis ^{2, ID}, D. Banerjee ^{4, ID}, Z. Banoo ^{90, ID}, R. Barbera ^{26, ID}, L. Barioglio ^{95, ID}, M. Barlou ⁷⁷, G.G. Barnaföldi ^{135, ID}, L.S. Barnby ^{84, ID}, V. Barret ^{123, ID}, L. Barreto ^{108, ID}, C. Bartels ^{115, ID}, K. Barth ^{32, ID}, E. Bartsch ^{63, ID}, F. Baruffaldi ^{27, ID}, N. Bastid ^{123, ID}, S. Basu ^{74, ID}, G. Batigne ^{102, ID}, D. Battistini ^{95, ID}, B. Batyunya ^{140, ID}, D. Bauri ⁴⁶, J.L. Bazo Alba ^{100, ID}, I.G. Bearden ^{82, ID}, C. Beattie ^{136, ID}, P. Becht ^{97, ID}, D. Behera ^{47, ID}, I. Belikov ^{125, ID}, A.D.C. Bell Hechavarria ^{134, ID}, F. Bellini ^{25, ID}, R. Bellwied ^{112, ID}, S. Belokurova ^{139, ID}, V. Belyaev ^{139, ID}, G. Bencedi ^{135,64, ID}, S. Beole ^{24, ID}, A. Bercuci ^{45, ID}, Y. Berdnikov ^{139, ID}, A. Berdnikova ^{94, ID}, L. Bergmann ^{94, ID}, M.G. Besouï ^{62, ID}, L. Betev ^{32, ID}, P.P. Bhaduri ^{131, ID}, A. Bhasin ^{90, ID}, I.R. Bhat ⁹⁰, M.A. Bhat ^{4, ID}, B. Bhattacharjee ^{41, ID}, L. Bianchi ^{24, ID}, N. Bianchi ^{48, ID}, J. Bielčík ^{35, ID}, J. Bielčíková ^{85, ID}, J. Biernat ^{105, ID}, A. Bilandžić ^{95, ID}, G. Biro ^{135, ID}, S. Biswas ^{4, ID}, J.T. Blair ^{106, ID}, D. Blau ^{139, ID}, M.B. Blidaru ^{97, ID}, N. Bluhme ³⁸, C. Blume ^{63, ID}, G. Boca ^{21,54, ID}, F. Bock ^{86, ID}, T. Bodova ^{20, ID}, A. Bogdanov ¹³⁹, S. Boi ^{22, ID}, J. Bok ^{57, ID}, L. Boldizsár ^{135, ID}, A. Bolozdynya ^{139, ID}, M. Bomba ^{37, ID}, P.M. Bond ^{32, ID}, G. Bonomi ^{130,54, ID}, H. Borel ^{126, ID}, A. Borissov ^{139, ID}, H. Bossi ^{136, ID}, E. Botta ^{24, ID}, L. Bratrud ^{63, ID}, P. Braun-Munzinger ^{97, ID}, M. Bregant ^{108, ID}, M. Broz ^{35, ID}, G.E. Bruno ^{96,31, ID}, M.D. Buckland ^{115, ID}, D. Budnikov ^{139, ID}, H. Buesching ^{63, ID}, S. Bufalino ^{29, ID}, O. Bugnon ¹⁰², P. Buhler ^{101, ID}, Z. Buthelezi ^{67,119, ID}, J.B. Butt ¹³, A. Bylinkin ^{114, ID}, S.A. Bysiak ¹⁰⁵, M. Cai ^{27,6, ID}, H. Caines ^{136, ID}, A. Caliva ^{97, ID}, E. Calvo Villar ^{100, ID}, J.M.M. Camacho ^{107, ID}, P. Camerini ^{23, ID}, F.D.M. Canedo ^{108, ID}, M. Carabas ^{122, ID}, F. Carnesecchi ^{32, ID}, R. Caron ^{124,126, ID}, J. Castillo Castellanos ^{126, ID}, F. Catalano ^{29, ID}, C. Ceballos Sanchez ^{140, ID}, I. Chakaberia ^{73, ID}, P. Chakraborty ^{46, ID}, S. Chandra ^{131, ID}, S. Chapelard ^{32, ID}, M. Chartier ^{115, ID}, S. Chattopadhyay ^{131, ID}, S. Chattopadhyay ^{98, ID}, T.G. Chavez ^{44, ID}, T. Cheng ^{6, ID}, C. Cheshkov ^{124, ID}, B. Cheynis ^{124, ID}, V. Chibante Barroso ^{32, ID}, D.D. Chinellato ^{109, ID}, E.S. Chizzali ^{95, ID}, J. Cho ^{57, ID}, S. Cho ^{57, ID}, P. Chochula ^{32, ID}, P. Christakoglou ^{83, ID}, C.H. Christensen ^{82, ID}, P. Christiansen ^{74, ID}, T. Chujo ^{121, ID}, M. Ciacco ^{29, ID}, C. Cicalo ^{51, ID}, L. Cifarelli ^{25, ID}, F. Cindolo ^{50, ID}, M.R. Ciupek ⁹⁷, G. Clai ^{50, III}, F. Colamaria ^{49, ID}, J.S. Colburn ⁹⁹, D. Colella ^{96,31, ID}, A. Collu ⁷³, M. Colocci ^{32, ID}, M. Concas ^{55, ID}, G. Conesa Balbastre ^{72, ID}, Z. Conesa del Valle ^{127, ID},

- G. Contin 23, [ID](#), J.G. Contreras 35, [ID](#), M.L. Coquet 126, [ID](#), T.M. Cormier 86, [I](#), P. Cortese 129, 55, [ID](#),
 M.R. Cosentino 110, [ID](#), F. Costa 32, [ID](#), S. Costanza 21, 54, [ID](#), P. Crochet 123, [ID](#), R. Cruz-Torres 73, [ID](#), E. Cuautle 64,
 P. Cui 6, [ID](#), L. Cunqueiro 86, A. Dainese 53, [ID](#), M.C. Danisch 94, [ID](#), A. Danu 62, [ID](#), P. Das 79, [ID](#), P. Das 4, [ID](#),
 S. Das 4, [ID](#), S. Dash 46, [ID](#), R.M.H. David 44, A. De Caro 28, [ID](#), G. de Cataldo 49, [ID](#), L. De Cilladi 24, [ID](#), J. de
 Cuveland 38, A. De Falco 22, [ID](#), D. De Gruttola 28, [ID](#), N. De Marco 55, [ID](#), C. De Martin 23, [ID](#), S. De
 Pasquale 28, [ID](#), S. Deb 47, [ID](#), H.F. Degenhardt 108, K.R. Deja 132, R. Del Grande 95, [ID](#), L. Dello Stritto 28, [ID](#),
 W. Deng 6, [ID](#), P. Dhankher 18, [ID](#), D. Di Bari 31, [ID](#), A. Di Mauro 32, [ID](#), R.A. Diaz 140, 7, [ID](#), T. Dietel 111, [ID](#),
 Y. Ding 124, 6, [ID](#), R. Divià 32, [ID](#), D.U. Dixit 18, [ID](#), Ø. Djupsland 20, U. Dmitrieva 139, [ID](#), A. Dobrin 62, [ID](#),
 B. Dönigus 63, [ID](#), A.K. Dubey 131, [ID](#), J.M. Dubinski 132, [ID](#), A. Dubla 97, [ID](#), S. Dudi 89, [ID](#), P. Dupieux 123, [ID](#),
 M. Durkac 104, N. Dzalaiova 12, T.M. Eder 134, [ID](#), R.J. Ehlers 86, [ID](#), V.N. Eikeland 20, F. Eisenhut 63, [ID](#),
 D. Elia 49, [ID](#), B. Erazmus 102, [ID](#), F. Ercolessi 25, [ID](#), F. Erhardt 88, [ID](#), M.R. Ersdal 20, B. Espagnon 127, [ID](#),
 G. Eulisse 32, [ID](#), D. Evans 99, [ID](#), S. Evdokimov 139, [ID](#), L. Fabbietti 95, [ID](#), M. Faggin 27, [ID](#), J. Faivre 72, [ID](#),
 F. Fan 6, [ID](#), W. Fan 73, [ID](#), A. Fantoni 48, [ID](#), M. Fasel 86, [ID](#), P. Fecchio 29, A. Feliciello 55, [ID](#), G. Feofilov 139, [ID](#),
 A. Fernández Téllez 44, [ID](#), M.B. Ferrer 32, [ID](#), A. Ferrero 126, [ID](#), A. Ferretti 24, [ID](#), V.J.G. Feuillard 94, [ID](#),
 J. Figiel 105, [ID](#), V. Filova 35, [ID](#), D. Finogeev 139, [ID](#), F.M. Fionda 51, [ID](#), G. Fiorenza 96, F. Flor 112, [ID](#),
 A.N. Flores 106, [ID](#), S. Foertsch 67, [ID](#), I. Fokin 94, [ID](#), S. Fokin 139, [ID](#), E. Fragiacomo 56, [ID](#), E. Frajna 135, [ID](#),
 U. Fuchs 32, [ID](#), N. Funicello 28, [ID](#), C. Furget 72, [ID](#), A. Furs 139, [ID](#), J.J. Gaardhøje 82, [ID](#), M. Gagliardi 24, [ID](#),
 A.M. Gago 100, [ID](#), A. Gal 125, C.D. Galvan 107, [ID](#), P. Ganoti 77, [ID](#), C. Garabatos 97, [ID](#), J.R.A. Garcia 44, [ID](#),
 E. Garcia-Solis 9, [ID](#), K. Garg 102, [ID](#), C. Gargiulo 32, [ID](#), A. Garibbi 80, K. Garner 134, E.F. Gauger 106, [ID](#),
 A. Gautam 114, [ID](#), M.B. Gay Ducati 65, [ID](#), M. Germain 102, [ID](#), S.K. Ghosh 4, M. Giacalone 25, [ID](#),
 P. Gianotti 48, [ID](#), P. Giubellino 97, 55, [ID](#), P. Giubilato 27, [ID](#), A.M.C. Glaenzer 126, [ID](#), P. Glässel 94, [ID](#),
 E. Glimos 118, [ID](#), D.J.Q. Goh 75, V. Gonzalez 133, [ID](#), L.H. González-Trueba 66, [ID](#), S. Gorbunov 38, [ID](#),
 M. Gorgon 2, [ID](#), L. Görlich 105, [ID](#), S. Gotovac 33, V. Grabski 66, [ID](#), L.K. Graczykowski 132, [ID](#), E. Grecka 85, [ID](#),
 L. Greiner 73, [ID](#), A. Grelli 58, [ID](#), C. Grigoras 32, [ID](#), V. Grigoriev 139, [ID](#), S. Grigoryan 140, 1, [ID](#), F. Grossa 32, [ID](#),
 J.F. Grosse-Oetringhaus 32, [ID](#), R. Grossi 97, [ID](#), D. Grund 35, [ID](#), G.G. Guardiano 109, [ID](#), R. Guernane 72, [ID](#),
 M. Guilbaud 102, [ID](#), K. Gulbrandsen 82, [ID](#), T. Gunji 120, [ID](#), W. Guo 6, [ID](#), A. Gupta 90, [ID](#), R. Gupta 90, [ID](#),
 S.P. Guzman 44, [ID](#), L. Gyulai 135, [ID](#), M.K. Habib 97, C. Hadjidakis 127, [ID](#), H. Hamagaki 75, [ID](#), M. Hamid 6, [ID](#),
 Y. Han 137, [ID](#), R. Hannigan 106, [ID](#), M.R. Haque 132, [ID](#), A. Harlenderova 97, J.W. Harris 136, [ID](#), A. Harton 9, [ID](#),
 J.A. Hasenbichler 32, H. Hassan 86, [ID](#), D. Hatzifotiadou 50, [ID](#), P. Hauer 42, [ID](#), L.B. Havener 136, [ID](#),
 S.T. Heckel 95, [ID](#), E. Hellbär 97, [ID](#), H. Helstrup 34, [ID](#), T. Herman 35, [ID](#), G. Herrera Corral 8, [ID](#), F. Herrmann 134, [ID](#),
 K.F. Hetland 34, [ID](#), B. Heybeck 63, [ID](#), H. Hillemanns 32, [ID](#), C. Hills 115, [ID](#), B. Hippolyte 125, [ID](#), B. Hofman 58, [ID](#),
 B. Hohlweger 83, [ID](#), J. Honermann 134, [ID](#), G.H. Hong 137, [ID](#), D. Horak 35, [ID](#), A. Horzyk 2, [ID](#), R. Hosokawa 14, [ID](#),
 Y. Hou 6, [ID](#), P. Hristov 32, [ID](#), C. Hughes 118, [ID](#), P. Huhn 63, L.M. Huhta 113, [ID](#), C.V. Hulse 127, [ID](#),
 T.J. Humanic 87, [ID](#), H. Hushnud 98, A. Hutson 112, [ID](#), D. Hutter 38, [ID](#), J.P. Iddon 115, [ID](#), R. Ilkaev 139, [ID](#),
 H. Ilyas 13, [ID](#), M. Inaba 121, [ID](#), G.M. Innocenti 32, [ID](#), M. Ippolitov 139, [ID](#), A. Isakov 85, [ID](#), T. Isidori 114, [ID](#),
 M.S. Islam 98, [ID](#), M. Ivanov 97, [ID](#), V. Ivanov 139, [ID](#), V. Izucheev 139, M. Jablonski 2, [ID](#), B. Jacak 73, [ID](#),
 N. Jacazio 32, [ID](#), P.M. Jacobs 73, [ID](#), S. Jadlovska 104, J. Jadlovsky 104, L. Jaffe 38, C. Jahnke 109, [ID](#),
 M.A. Janik 132, [ID](#), T. Janson 69, M. Jercic 88, O. Jevons 99, A.A.P. Jimenez 64, [ID](#), F. Jonas 86, [ID](#), P.G. Jones 99, [ID](#),
 J.M. Jowett 32, 97, [ID](#), J. Jung 63, [ID](#), M. Jung 63, [ID](#), A. Junique 32, [ID](#), A. Jusko 99, [ID](#), M.J. Kabus 32, 132, [ID](#),
 J. Kaewjai 103, P. Kalinak 59, [ID](#), A.S. Kalteyer 97, [ID](#), A. Kalweit 32, [ID](#), V. Kaplin 139, [ID](#), A. Karasu Uysal 71, [ID](#),
 D. Karatovic 88, [ID](#), O. Karavichev 139, [ID](#), T. Karavicheva 139, [ID](#), P. Karczmarczyk 132, [ID](#), E. Karpechev 139, [ID](#),
 V. Kashyap 79, A. Kazantsev 139, U. Kebschull 69, [ID](#), R. Keidel 138, [ID](#), D.L.D. Keijdener 58, M. Keil 32, [ID](#),

- B. Ketzer ^{42, ID}, A.M. Khan ^{6, ID}, S. Khan ^{15, ID}, A. Khanzadeev ^{139, ID}, Y. Kharlov ^{139, ID}, A. Khatun ^{15, ID},
 A. Khuntia ^{105, ID}, B. Kileng ^{34, ID}, B. Kim ^{16, ID}, C. Kim ^{16, ID}, D.J. Kim ^{113, ID}, E.J. Kim ^{68, ID}, J. Kim ^{137, ID},
 J.S. Kim ^{40, ID}, J. Kim ^{94, ID}, J. Kim ^{68, ID}, M. Kim ^{94, ID}, S. Kim ^{17, ID}, T. Kim ^{137, ID}, S. Kirsch ^{63, ID}, I. Kisel ^{38, ID},
 S. Kiselev ^{139, ID}, A. Kisiel ^{132, ID}, J.P. Kitowski ^{2, ID}, J.L. Klay ^{5, ID}, J. Klein ^{32, ID}, S. Klein ^{73, ID},
 C. Klein-Bösing ^{134, ID}, M. Kleiner ^{63, ID}, T. Klemenz ^{95, ID}, A. Kluge ^{32, ID}, A.G. Knospe ^{112, ID}, C. Kobdaj ^{103, ID},
 T. Kollegger ⁹⁷, A. Kondratyev ^{140, ID}, N. Kondratyeva ^{139, ID}, E. Kondratyuk ^{139, ID}, J. Konig ^{63, ID},
 S.A. Konigstorfer ^{95, ID}, P.J. Konopka ^{32, ID}, G. Kornakov ^{132, ID}, S.D. Koryciak ^{2, ID}, A. Kotliarov ^{85, ID},
 O. Kovalenko ^{78, ID}, V. Kovalenko ^{139, ID}, M. Kowalski ^{105, ID}, I. Králik ^{59, ID}, A. Kravčáková ^{37, ID}, L. Kreis ⁹⁷,
 M. Krivda ^{99, 59, ID}, F. Krizek ^{85, ID}, K. Krizkova Gajdosova ^{35, ID}, M. Kroesen ^{94, ID}, M. Krüger ^{63, ID},
 D.M. Krupova ^{35, ID}, E. Kryshen ^{139, ID}, M. Krzewicki ³⁸, V. Kučera ^{32, ID}, C. Kuhn ^{125, ID}, P.G. Kuijer ^{83, ID},
 T. Kumaoka ¹²¹, D. Kumar ¹³¹, L. Kumar ^{89, ID}, N. Kumar ⁸⁹, S. Kundu ^{32, ID}, P. Kurashvili ^{78, ID},
 A. Kurepin ^{139, ID}, A.B. Kurepin ^{139, ID}, S. Kushpil ^{85, ID}, J. Kvapil ^{99, ID}, M.J. Kweon ^{57, ID}, J.Y. Kwon ^{57, ID},
 Y. Kwon ^{137, ID}, S.L. La Pointe ^{38, ID}, P. La Rocca ^{26, ID}, Y.S. Lai ⁷³, A. Lakrathok ¹⁰³, M. Lamanna ^{32, ID},
 R. Langoy ^{117, ID}, P. Larionov ^{48, ID}, E. Laudi ^{32, ID}, L. Lautner ^{32, 95, ID}, R. Lavicka ^{101, ID}, T. Lazareva ^{139, ID},
 R. Lea ^{130, 54, ID}, J. Lehrbach ^{38, ID}, R.C. Lemmon ^{84, ID}, I. León Monzón ^{107, ID}, M.M. Lesch ^{95, ID},
 E.D. Lesser ^{18, ID}, M. Lettrich ⁹⁵, P. Lévai ^{135, ID}, X. Li ¹⁰, X.L. Li ⁶, J. Lien ^{117, ID}, R. Lietava ^{99, ID}, B. Lim ^{16, ID},
 S.H. Lim ^{16, ID}, V. Lindenstruth ^{38, ID}, A. Lindner ⁴⁵, C. Lippmann ^{97, ID}, A. Liu ^{18, ID}, D.H. Liu ^{6, ID}, J. Liu ^{115, ID},
 I.M. Lofnes ^{20, ID}, V. Loginov ¹³⁹, C. Loizides ^{86, ID}, P. Loncar ^{33, ID}, J.A. Lopez ^{94, ID}, X. Lopez ^{123, ID}, E. López
 Torres ^{7, ID}, P. Lu ^{97, 116, ID}, J.R. Luhder ^{134, ID}, M. Lunardon ^{27, ID}, G. Luparello ^{56, ID}, Y.G. Ma ^{39, ID},
 A. Maevskaya ¹³⁹, M. Mager ^{32, ID}, T. Mahmoud ⁴², A. Maire ^{125, ID}, M. Malaev ^{139, ID}, N.M. Malik ^{90, ID},
 Q.W. Malik ¹⁹, S.K. Malik ^{90, ID}, L. Malinina ^{140, ID, I, VII}, D. Mal'Kevich ^{139, ID}, D. Mallick ^{79, ID}, N. Mallick ^{47, ID},
 G. Mandaglio ^{30, 52, ID}, V. Manko ^{139, ID}, F. Manso ^{123, ID}, V. Manzari ^{49, ID}, Y. Mao ^{6, ID}, G.V. Margagliotti ^{23, ID},
 A. Margotti ^{50, ID}, A. Marín ^{97, ID}, C. Markert ^{106, ID}, M. Marquard ⁶³, N.A. Martin ⁹⁴, P. Martinengo ^{32, ID},
 J.L. Martinez ¹¹², M.I. Martínez ^{44, ID}, G. Martínez García ^{102, ID}, S. Masciocchi ^{97, ID}, M. Masera ^{24, ID},
 A. Masoni ^{51, ID}, L. Massacrier ^{127, ID}, A. Mastroserio ^{128, 49, ID}, A.M. Mathis ^{95, ID}, O. Matonoha ^{74, ID},
 P.F.T. Matuoka ¹⁰⁸, A. Matyja ^{105, ID}, C. Mayer ^{105, ID}, A.L. Mazuecos ^{32, ID}, F. Mazzaschi ^{24, ID},
 M. Mazzilli ^{32, ID}, J.E. Mdhluli ^{119, ID}, A.F. Mechler ⁶³, Y. Melikyan ^{139, ID}, A. Menchaca-Rocha ^{66, ID},
 E. Meninno ^{101, 28, ID}, A.S. Menon ^{112, ID}, M. Meres ^{12, ID}, S. Mhlanga ^{111, 67}, Y. Miake ¹²¹, L. Micheletti ^{55, ID},
 L.C. Migliorin ¹²⁴, D.L. Mihaylov ^{95, ID}, K. Mikhaylov ^{140, 139, ID}, A.N. Mishra ^{135, ID}, D. Miśkowiec ^{97, ID},
 A. Modak ^{4, ID}, A.P. Mohanty ^{58, ID}, B. Mohanty ⁷⁹, M. Mohisin Khan ^{15, ID, V}, M.A. Molander ^{43, ID},
 Z. Moravcová ^{82, ID}, C. Mordasini ^{95, ID}, D.A. Moreira De Godoy ^{134, ID}, I. Morozov ^{139, ID}, A. Morsch ^{32, ID},
 T. Mrnjavac ^{32, ID}, V. Muccifora ^{48, ID}, E. Mudnic ³³, S. Muhuri ^{131, ID}, J.D. Mulligan ^{73, ID}, A. Mulliri ²²,
 M.G. Munhoz ^{108, ID}, R.H. Munzer ^{63, ID}, H. Murakami ^{120, ID}, S. Murray ^{111, ID}, L. Musa ^{32, ID},
 J. Musinsky ^{59, ID}, J.W. Myrcha ^{132, ID}, B. Naik ^{119, ID}, R. Nair ^{78, ID}, B.K. Nandi ^{46, ID}, R. Nania ^{50, ID},
 E. Nappi ^{49, ID}, A.F. Nassirpour ^{74, ID}, A. Nath ^{94, ID}, C. Nattrass ^{118, ID}, A. Neagu ¹⁹, A. Negru ¹²²,
 L. Nellen ^{64, ID}, S.V. Nesbo ³⁴, G. Neskovic ^{38, ID}, D. Nesterov ^{139, ID}, B.S. Nielsen ^{82, ID}, E.G. Nielsen ^{82, ID},
 S. Nikolaev ^{139, ID}, S. Nikulin ^{139, ID}, V. Nikulin ^{139, ID}, F. Noferini ^{50, ID}, S. Noh ^{11, ID}, P. Nomokonov ^{140, ID},
 J. Norman ^{115, ID}, N. Novitzky ^{121, ID}, P. Nowakowski ^{132, ID}, A. Nyanin ^{139, ID}, J. Nystrand ^{20, ID},
 M. Ogino ^{75, ID}, A. Ohlson ^{74, ID}, V.A. Okorokov ^{139, ID}, J. Oleniacz ^{132, ID}, A.C. Oliveira Da Silva ^{118, ID},
 M.H. Oliver ^{136, ID}, A. Onnerstad ^{113, ID}, C. Oppedisano ^{55, ID}, A. Ortiz Velasquez ^{64, ID}, A. Oskarsson ⁷⁴,
 J. Otwinowski ^{105, ID}, M. Oya ⁹², K. Oyama ^{75, ID}, Y. Pachmayer ^{94, ID}, S. Padhan ^{46, ID}, D. Pagano ^{130, 54, ID},
 G. Paić ^{64, ID}, A. Palasciano ^{49, ID}, S. Panebianco ^{126, ID}, J. Park ^{57, ID}, J.E. Parkkila ^{32, 113, ID}, S.P. Pathak ¹¹²,

- R.N. Patra ⁹⁰, B. Paul ^{22, ID}, H. Pei ^{6, ID}, T. Peitzmann ^{58, ID}, X. Peng ^{6, ID}, L.G. Pereira ^{65, ID}, H. Pereira Da Costa ^{126, ID}, D. Peresunko ^{139, ID}, G.M. Perez ^{7, ID}, S. Perrin ^{126, ID}, Y. Pestov ¹³⁹, V. Petráček ^{35, ID}, V. Petrov ^{139, ID}, M. Petrovici ^{45, ID}, R.P. Pezzi ^{102, 65, ID}, S. Piano ^{56, ID}, M. Pikna ^{12, ID}, P. Pillot ^{102, ID}, O. Pinazza ^{50, 32, ID}, L. Pinsky ¹¹², C. Pinto ^{95, 26, ID}, S. Pisano ^{48, ID}, M. Płoskoń ^{73, ID}, M. Planinic ⁸⁸, F. Pliquet ⁶³, M.G. Poghosyan ^{86, ID}, S. Politano ^{29, ID}, N. Poljak ^{88, ID}, A. Pop ^{45, ID}, S. Porteboeuf-Houssais ^{123, ID}, J. Porter ^{73, ID}, V. Pozdniakov ^{140, ID}, S.K. Prasad ^{4, ID}, S. Prasad ^{47, ID}, R. Preghenella ^{50, ID}, F. Prino ^{55, ID}, C.A. Pruneau ^{133, ID}, I. Pshenichnov ^{139, ID}, M. Puccio ^{32, ID}, S. Qiu ^{83, ID}, L. Quaglia ^{24, ID}, R.E. Quishpe ¹¹², S. Ragoni ^{99, ID}, A. Rakotozafindrabe ^{126, ID}, L. Ramello ^{129, 55, ID}, F. Rami ^{125, ID}, S.A.R. Ramirez ^{44, ID}, T.A. Rancien ⁷², R. Raniwala ^{91, ID}, S. Raniwala ⁹¹, S.S. Räsänen ^{43, ID}, R. Rath ^{47, ID}, I. Ravasenga ^{83, ID}, K.F. Read ^{86, 118, ID}, A.R. Redelbach ^{38, ID}, K. Redlich ^{78, ID, VI}, A. Rehman ²⁰, P. Reichelt ⁶³, F. Reidt ^{32, ID}, H.A. Reme-Ness ^{34, ID}, Z. Rescakova ³⁷, K. Reygers ^{94, ID}, A. Riabov ^{139, ID}, V. Riabov ^{139, ID}, R. Ricci ^{28, ID}, T. Richert ⁷⁴, M. Richter ^{19, ID}, W. Riegler ^{32, ID}, F. Riggi ^{26, ID}, C. Ristea ^{62, ID}, M. Rodríguez Cahuantzi ^{44, ID}, K. Røed ^{19, ID}, R. Rogalev ^{139, ID}, E. Rogochaya ^{140, ID}, T.S. Rogoschinski ^{63, ID}, D. Rohr ^{32, ID}, D. Röhrich ^{20, ID}, P.F. Rojas ⁴⁴, S. Rojas Torres ^{35, ID}, P.S. Rokita ^{132, ID}, F. Ronchetti ^{48, ID}, A. Rosano ^{30, 52, ID}, E.D. Rosas ⁶⁴, A. Rossi ^{53, ID}, A. Roy ^{47, ID}, P. Roy ⁹⁸, S. Roy ^{46, ID}, N. Rubini ^{25, ID}, D. Ruggiano ^{132, ID}, R. Rui ^{23, ID}, B. Rumyantsev ¹⁴⁰, P.G. Russek ^{2, ID}, R. Russo ^{83, ID}, A. Rustamov ^{80, ID}, E. Ryabinkin ^{139, ID}, Y. Ryabov ^{139, ID}, A. Rybicki ^{105, ID}, H. Rytkonen ^{113, ID}, W. Rzesz ^{132, ID}, O.A.M. Saarimaki ^{43, ID}, R. Sadek ^{102, ID}, S. Sadovsky ^{139, ID}, J. Saetre ^{20, ID}, K. Šafařík ^{35, ID}, S.K. Saha ^{131, ID}, S. Saha ^{79, ID}, B. Sahoo ^{46, ID}, P. Sahoo ⁴⁶, R. Sahoo ^{47, ID}, S. Sahoo ⁶⁰, D. Sahu ^{47, ID}, P.K. Sahu ^{60, ID}, J. Saini ^{131, ID}, K. Sajdakova ³⁷, S. Sakai ^{121, ID}, M.P. Salvan ^{97, ID}, S. Sambyal ^{90, ID}, T.B. Saramela ¹⁰⁸, D. Sarkar ^{133, ID}, N. Sarkar ¹³¹, P. Sarma ^{41, ID}, V. Sarritzu ^{22, ID}, V.M. Sarti ^{95, ID}, M.H.P. Sas ^{136, ID}, J. Schambach ^{86, ID}, H.S. Scheid ^{63, ID}, C. Schiaua ^{45, ID}, R. Schicker ^{94, ID}, A. Schmah ⁹⁴, C. Schmidt ^{97, ID}, H.R. Schmidt ⁹³, M.O. Schmidt ^{32, ID}, M. Schmidt ⁹³, N.V. Schmidt ^{86, 63, ID}, A.R. Schmier ^{118, ID}, R. Schotter ^{125, ID}, J. Schukraft ^{32, ID}, K. Schwarz ⁹⁷, K. Schweda ^{97, ID}, G. Scioli ^{25, ID}, E. Scomparin ^{55, ID}, J.E. Seger ^{14, ID}, Y. Sekiguchi ¹²⁰, D. Sekihata ^{120, ID}, I. Selyuzhenkov ^{97, 139, ID}, S. Senyukov ^{125, ID}, J.J. Seo ^{57, ID}, D. Serebryakov ^{139, ID}, L. Šerkšnytė ^{95, ID}, A. Sevcenco ^{62, ID}, T.J. Shaba ^{67, ID}, A. Shabanov ¹³⁹, A. Shabetai ^{102, ID}, R. Shahoyan ³², W. Shaikh ⁹⁸, A. Shangaraev ^{139, ID}, A. Sharma ⁸⁹, D. Sharma ^{46, ID}, H. Sharma ^{105, ID}, M. Sharma ^{90, ID}, N. Sharma ^{89, ID}, S. Sharma ^{90, ID}, U. Sharma ^{90, ID}, A. Shatat ^{127, ID}, O. Sheibani ¹¹², K. Shigaki ^{92, ID}, M. Shimomura ⁷⁶, S. Shirinkin ^{139, ID}, Q. Shou ^{39, ID}, Y. Sibirskiak ^{139, ID}, S. Siddhanta ^{51, ID}, T. Siemiaczuk ^{78, ID}, T.F. Silva ^{108, ID}, D. Silvermyr ^{74, ID}, T. Simantathammakul ¹⁰³, R. Simeonov ^{36, ID}, G. Simonetti ³², B. Singh ⁹⁰, B. Singh ^{95, ID}, R. Singh ^{79, ID}, R. Singh ^{90, ID}, R. Singh ^{47, ID}, V.K. Singh ^{131, ID}, V. Singhal ^{131, ID}, T. Sinha ^{98, ID}, B. Sitar ^{12, ID}, M. Sitta ^{129, 55, ID}, T.B. Skaali ¹⁹, G. Skorodumovs ^{94, ID}, M. Slupecki ^{43, ID}, N. Smirnov ^{136, ID}, R.J.M. Snellings ^{58, ID}, E.H. Solheim ^{19, ID}, C. Soncco ¹⁰⁰, J. Song ^{112, ID}, A. Songmoolnak ¹⁰³, F. Soramel ^{27, ID}, S.P. Sorensen ^{118, ID}, R. Soto Camacho ⁴⁴, R. Spijkers ^{83, ID}, I. Sputowska ^{105, ID}, J. Staa ^{74, ID}, J. Stachel ^{94, ID}, I. Stan ^{62, ID}, P.J. Steffanic ^{118, ID}, S.F. Stiefelmaier ^{94, ID}, D. Stocco ^{102, ID}, I. Storehaug ^{19, ID}, M.M. Storetvedt ^{34, ID}, P. Stratmann ^{134, ID}, S. Strazzi ^{25, ID}, C.P. Stylianidis ⁸³, A.A.P. Suaiide ^{108, ID}, C. Suire ^{127, ID}, M. Sukhanov ^{139, ID}, M. Suljic ^{32, ID}, V. Sumberia ^{90, ID}, S. Sumowidagdo ^{81, ID}, S. Swain ⁶⁰, A. Szabo ¹², I. Szarka ^{12, ID}, U. Tabassam ¹³, S.F. Taghavi ^{95, ID}, G. Taillepied ^{97, 123, ID}, J. Takahashi ^{109, ID}, G.J. Tambave ^{20, ID}, S. Tang ^{123, 6, ID}, Z. Tang ^{116, ID}, J.D. Tapia Takaki ^{114, ID}, N. Tapus ¹²², L.A. Tarasovicova ^{134, ID}, M.G. Tarzila ^{45, ID}, A. Tauro ^{32, ID}, A. Telesca ^{32, ID}, L. Terlizzi ^{24, ID}, C. Terrevoli ^{112, ID}, G. Tersimonov ³, S. Thakur ^{131, ID}, D. Thomas ^{106, ID}, R. Tieulent ^{124, ID}, A. Tikhonov ^{139, ID}, A.R. Timmins ^{112, ID}, M. Tkacik ¹⁰⁴, T. Tkacik ^{104, ID},

- A. Toia^{63, ID}, N. Topilskaya^{139, ID}, M. Toppi^{48, ID}, F. Torales-Acosta¹⁸, T. Tork^{127, ID}, A.G. Torres Ramos^{31, ID}, A. Trifiró^{30,52, ID}, A.S. Triolo^{30,52, ID}, S. Tripathy^{50, ID}, T. Tripathy^{46, ID}, S. Trogolo^{32, ID}, V. Trubnikov^{3, ID}, W.H. Trzaska^{113, ID}, T.P. Trzcinski^{132, ID}, R. Turrisi^{53, ID}, T.S. Tveter^{19, ID}, K. Ullaland^{20, ID}, B. Ulukutlu^{95, ID}, A. Uras^{124, ID}, M. Urioni^{54, 130, ID}, G.L. Usai^{22, ID}, M. Vala³⁷, N. Valle^{21, ID}, S. Vallero^{55, ID}, L.V.R. van Doremalen⁵⁸, M. van Leeuwen^{83, ID}, C.A. van Veen^{94, ID}, R.J.G. van Weelden^{83, ID}, P. Vande Vyvre^{32, ID}, D. Varga^{135, ID}, Z. Varga^{135, ID}, M. Varga-Kofarago^{135, ID}, M. Vasileiou^{77, ID}, A. Vasiliev^{139, ID}, O. Vázquez Doce^{95, ID}, O. Vazquez Rueda^{74, ID}, V. Vechernin^{139, ID}, E. Vercellin^{24, ID}, S. Vergara Limón⁴⁴, L. Vermunt^{58, ID}, R. Vértesi^{135, ID}, M. Verweij^{58, ID}, L. Vickovic³³, Z. Vilakazi¹¹⁹, O. Villalobos Baillie^{99, ID}, G. Vino^{49, ID}, A. Vinogradov^{139, ID}, T. Virgili^{28, ID}, V. Vislavicius⁸², A. Vodopyanov^{140, ID}, B. Volkel^{32, ID}, M.A. Völkl^{94, ID}, K. Voloshin¹³⁹, S.A. Voloshin^{133, ID}, G. Volpe^{31, ID}, B. von Haller^{32, ID}, I. Vorobyev^{95, ID}, N. Vozniuk^{139, ID}, J. Vrláková^{37, ID}, B. Wagner²⁰, C. Wang^{39, ID}, D. Wang³⁹, M. Weber^{101, ID}, A. Wegrzynek^{32, ID}, F.T. Weiglhofer³⁸, S.C. Wenzel^{32, ID}, J.P. Wessels^{134, ID}, S.L. Weyhmiller^{136, ID}, J. Wiechula^{63, ID}, J. Wikne^{19, ID}, G. Wilk^{78, ID}, J. Wilkinson^{97, ID}, G.A. Willems^{134, ID}, B. Windelband^{94, ID}, M. Winn^{126, ID}, J.R. Wright^{106, ID}, W. Wu³⁹, Y. Wu^{116, ID}, R. Xu^{6, ID}, A.K. Yadav^{131, ID}, S. Yalcin^{71, ID}, Y. Yamaguchi^{92, ID}, K. Yamakawa⁹², S. Yang²⁰, S. Yano^{92, ID}, Z. Yin^{6, ID}, I.-K. Yoo^{16, ID}, J.H. Yoon^{57, ID}, S. Yuan²⁰, A. Yuncu^{94, ID}, V. Zaccolo^{23, ID}, C. Zampolli^{32, ID}, H.J.C. Zanolli⁵⁸, F. Zanone^{94, ID}, N. Zardoshti^{32,99, ID}, A. Zarochentsev^{139, ID}, P. Závada^{61, ID}, N. Zaviyalov¹³⁹, M. Zhalov^{139, ID}, B. Zhang^{6, ID}, S. Zhang^{39, ID}, X. Zhang^{6, ID}, Y. Zhang¹¹⁶, M. Zhao^{10, ID}, V. Zherebchevskii^{139, ID}, Y. Zhi¹⁰, N. Zhigareva¹³⁹, D. Zhou^{6, ID}, Y. Zhou^{82, ID}, J. Zhu^{97,6, ID}, Y. Zhu⁶, G. Zinovjev^{3,I}, N. Zurlo^{130,54, ID}

¹ A.I. Alikhanyan National Science Laboratory (Yerevan Physics Institute) Foundation, Yerevan, Armenia² AGH University of Krakow, Cracow, Poland³ Bogolyubov Institute for Theoretical Physics, National Academy of Sciences of Ukraine, Kiev, Ukraine⁴ Bose Institute, Department of Physics and Centre for Astroparticle Physics and Space Science (CAPSS), Kolkata, India⁵ California Polytechnic State University, San Luis Obispo, CA, United States⁶ Central China Normal University, Wuhan, China⁷ Centro de Aplicaciones Tecnológicas y Desarrollo Nuclear (CEADEN), Havana, Cuba⁸ Centro de Investigación y de Estudios Avanzados (CINVESTAV), Mexico City and Mérida, Mexico⁹ Chicago State University, Chicago, IL, United States¹⁰ China Institute of Atomic Energy, Beijing, China¹¹ Chungbuk National University, Cheongju, Republic of Korea¹² Comenius University Bratislava, Faculty of Mathematics, Physics and Informatics, Bratislava, Slovak Republic¹³ COMSATS University Islamabad, Islamabad, Pakistan¹⁴ Creighton University, Omaha, NE, United States¹⁵ Department of Physics, Aligarh Muslim University, Aligarh, India¹⁶ Department of Physics, Pusan National University, Pusan, Republic of Korea¹⁷ Department of Physics, Sejong University, Seoul, Republic of Korea¹⁸ Department of Physics, University of California, Berkeley, CA, United States¹⁹ Department of Physics, University of Oslo, Oslo, Norway²⁰ Department of Physics and Technology, University of Bergen, Bergen, Norway²¹ Dipartimento di Fisica, Università di Pavia, Pavia, Italy²² Dipartimento di Fisica dell'Università e Sezione INFN, Cagliari, Italy²³ Dipartimento di Fisica dell'Università e Sezione INFN, Trieste, Italy²⁴ Dipartimento di Fisica dell'Università e Sezione INFN, Turin, Italy²⁵ Dipartimento di Fisica e Astronomia dell'Università e Sezione INFN, Bologna, Italy²⁶ Dipartimento di Fisica e Astronomia dell'Università e Sezione INFN, Catania, Italy²⁷ Dipartimento di Fisica e Astronomia dell'Università e Sezione INFN, Padova, Italy²⁸ Dipartimento di Fisica 'E.R. Caianiello' dell'Università e Gruppo Collegato INFN, Salerno, Italy²⁹ Dipartimento DISAT del Politecnico e Sezione INFN, Turin, Italy³⁰ Dipartimento di Scienze MIFT, Università di Messina, Messina, Italy³¹ Dipartimento Interateneo di Fisica 'M. Merlin' e Sezione INFN, Bari, Italy³² European Organization for Nuclear Research (CERN), Geneva, Switzerland³³ Faculty of Electrical Engineering, Mechanical Engineering and Naval Architecture, University of Split, Split, Croatia³⁴ Faculty of Engineering and Science, Western Norway University of Applied Sciences, Bergen, Norway³⁵ Faculty of Nuclear Sciences and Physical Engineering, Czech Technical University in Prague, Prague, Czech Republic³⁶ Faculty of Physics, Sofia University, Sofia, Bulgaria³⁷ Faculty of Science, P.J. Šafárik University, Košice, Slovak Republic³⁸ Frankfurt Institute for Advanced Studies, Johann Wolfgang Goethe-Universität Frankfurt, Frankfurt, Germany³⁹ Fudan University, Shanghai, China⁴⁰ Gangneung-Wonju National University, Gangneung, Republic of Korea⁴¹ Gauhati University, Department of Physics, Guwahati, India⁴² Helmholtz-Institut für Strahlen- und Kernphysik, Rheinische Friedrich-Wilhelms-Universität Bonn, Bonn, Germany⁴³ Helsinki Institute of Physics (HIP), Helsinki, Finland

- ⁴⁴ High Energy Physics Group, Universidad Autónoma de Puebla, Puebla, Mexico
⁴⁵ Horia Hulubei National Institute of Physics and Nuclear Engineering, Bucharest, Romania
⁴⁶ Indian Institute of Technology Bombay (IIT), Mumbai, India
⁴⁷ Indian Institute of Technology Indore, Indore, India
⁴⁸ INFN, Laboratori Nazionali di Frascati, Frascati, Italy
⁴⁹ INFN, Sezione di Bari, Bari, Italy
⁵⁰ INFN, Sezione di Bologna, Bologna, Italy
⁵¹ INFN, Sezione di Cagliari, Cagliari, Italy
⁵² INFN, Sezione di Catania, Catania, Italy
⁵³ INFN, Sezione di Padova, Padova, Italy
⁵⁴ INFN, Sezione di Pavia, Pavia, Italy
⁵⁵ INFN, Sezione di Torino, Turin, Italy
⁵⁶ INFN, Sezione di Trieste, Trieste, Italy
⁵⁷ Inha University, Incheon, Republic of Korea
⁵⁸ Institute for Gravitational and Subatomic Physics (GRASP), Utrecht University/Nikhef, Utrecht, Netherlands
⁵⁹ Institute of Experimental Physics, Slovak Academy of Sciences, Košice, Slovak Republic
⁶⁰ Institute of Physics, Homi Bhabha National Institute, Bhubaneswar, India
⁶¹ Institute of Physics of the Czech Academy of Sciences, Prague, Czech Republic
⁶² Institute of Space Science (ISS), Bucharest, Romania
⁶³ Institut für Kernphysik, Johann Wolfgang Goethe-Universität Frankfurt, Frankfurt, Germany
⁶⁴ Instituto de Ciencias Nucleares, Universidad Nacional Autónoma de México, Mexico City, Mexico
⁶⁵ Instituto de Física, Universidade Federal do Rio Grande do Sul (UFRGS), Porto Alegre, Brazil
⁶⁶ Instituto de Física, Universidad Nacional Autónoma de México, Mexico City, Mexico
⁶⁷ iThemba LABS, National Research Foundation, Somerset West, South Africa
⁶⁸ Jeonbuk National University, Jeonju, Republic of Korea
⁶⁹ Johann-Wolfgang-Goethe Universität Frankfurt Institut für Informatik, Fachbereich Informatik und Mathematik, Frankfurt, Germany
⁷⁰ Korea Institute of Science and Technology Information, Daejeon, Republic of Korea
⁷¹ KTO Karatay University, Konya, Turkey
⁷² Laboratoire de Physique Subatomique et de Cosmologie, Université Grenoble-Alpes, CNRS-IN2P3, Grenoble, France
⁷³ Lawrence Berkeley National Laboratory, Berkeley, CA, United States
⁷⁴ Lund University Department of Physics, Division of Particle Physics, Lund, Sweden
⁷⁵ Nagasaki Institute of Applied Science, Nagasaki, Japan
⁷⁶ Nara Women's University (NWU), Nara, Japan
⁷⁷ National and Kapodistrian University of Athens, School of Science, Department of Physics, Athens, Greece
⁷⁸ National Centre for Nuclear Research, Warsaw, Poland
⁷⁹ National Institute of Science Education and Research, Homi Bhabha National Institute, Jatni, India
⁸⁰ National Nuclear Research Center, Baku, Azerbaijan
⁸¹ National Research and Innovation Agency - BRIN, Jakarta, Indonesia
⁸² Niels Bohr Institute, University of Copenhagen, Copenhagen, Denmark
⁸³ Nikhef, National institute for subatomic physics, Amsterdam, Netherlands
⁸⁴ Nuclear Physics Group, STFC Daresbury Laboratory, Daresbury, United Kingdom
⁸⁵ Nuclear Physics Institute of the Czech Academy of Sciences, Husinec-Řež, Czech Republic
⁸⁶ Oak Ridge National Laboratory, Oak Ridge, TN, United States
⁸⁷ Ohio State University, Columbus, OH, United States
⁸⁸ Physics department, Faculty of science, University of Zagreb, Zagreb, Croatia
⁸⁹ Physics Department, Panjab University, Chandigarh, India
⁹⁰ Physics Department, University of Jammu, Jammu, India
⁹¹ Physics Department, University of Rajasthan, Jaipur, India
⁹² Physics Program and International Institute for Sustainability with Knotted Chiral Meta Matter (SKCM2), Hiroshima University, Hiroshima, Japan
⁹³ Physikalisches Institut, Eberhard-Karls-Universität Tübingen, Tübingen, Germany
⁹⁴ Physikalisches Institut, Ruprecht-Karls-Universität Heidelberg, Heidelberg, Germany
⁹⁵ Physik Department, Technische Universität München, Munich, Germany
⁹⁶ Politecnico di Bari and Sezione INFN, Bari, Italy
⁹⁷ Research Division and ExtreMe Matter Institute EMMI, GSI Helmholtzzentrum für Schwerionenforschung GmbH, Darmstadt, Germany
⁹⁸ Saha Institute of Nuclear Physics, Homi Bhabha National Institute, Kolkata, India
⁹⁹ School of Physics and Astronomy, University of Birmingham, Birmingham, United Kingdom
¹⁰⁰ Sección Física, Departamento de Ciencias, Pontificia Universidad Católica del Perú, Lima, Peru
¹⁰¹ Stefan Meyer Institut für Subatomare Physik (SMI), Vienna, Austria
¹⁰² SUBATECH, IMT Atlantique, Nantes Université, CNRS-IN2P3, Nantes, France
¹⁰³ Suranaree University of Technology, Nakhon Ratchasima, Thailand
¹⁰⁴ Technical University of Košice, Košice, Slovak Republic
¹⁰⁵ The Henryk Niewodniczanski Institute of Nuclear Physics, Polish Academy of Sciences, Cracow, Poland
¹⁰⁶ The University of Texas at Austin, Austin, TX, United States
¹⁰⁷ Universidad Autónoma de Sinaloa, Culiacán, Mexico
¹⁰⁸ Universidade de São Paulo (USP), São Paulo, Brazil
¹⁰⁹ Universidade Estadual de Campinas (UNICAMP), Campinas, Brazil
¹¹⁰ Universidade Federal do ABC, Santo André, Brazil
¹¹¹ University of Cape Town, Cape Town, South Africa
¹¹² University of Houston, Houston, TX, United States
¹¹³ University of Jyväskylä, Jyväskylä, Finland
¹¹⁴ University of Kansas, Lawrence, KS, United States
¹¹⁵ University of Liverpool, Liverpool, United Kingdom
¹¹⁶ University of Science and Technology of China, Hefei, China
¹¹⁷ University of South-Eastern Norway, Kongsberg, Norway
¹¹⁸ University of Tennessee, Knoxville, TN, United States
¹¹⁹ University of the Witwatersrand, Johannesburg, South Africa
¹²⁰ University of Tokyo, Tokyo, Japan
¹²¹ University of Tsukuba, Tsukuba, Japan
¹²² University Politehnica of Bucharest, Bucharest, Romania
¹²³ Université Clermont Auvergne, CNRS/IN2P3, LPC, Clermont-Ferrand, France

- ¹²⁴ Université de Lyon, CNRS/IN2P3, Institut de Physique des 2 Infinis de Lyon, Lyon, France
¹²⁵ Université de Strasbourg, CNRS, IPHC UMR 7178, F-67000, Strasbourg, France
¹²⁶ Université Paris-Saclay, Centre d'Etudes de Saclay (CEA), IRFU, Département de Physique Nucléaire (DPhN), Saclay, France
¹²⁷ Université Paris-Saclay, CNRS/IN2P3, IJCLab, Orsay, France
¹²⁸ Università degli Studi di Foggia, Foggia, Italy
¹²⁹ Università del Piemonte Orientale, Vercelli, Italy
¹³⁰ Università di Brescia, Brescia, Italy
¹³¹ Variable Energy Cyclotron Centre, Homi Bhabha National Institute, Kolkata, India
¹³² Warsaw University of Technology, Warsaw, Poland
¹³³ Wayne State University, Detroit, MI, United States
¹³⁴ Westfälische Wilhelms-Universität Münster, Institut für Kernphysik, Münster, Germany
¹³⁵ Wigner Research Centre for Physics, Budapest, Hungary
¹³⁶ Yale University, New Haven, CT, United States
¹³⁷ Yonsei University, Seoul, Republic of Korea
¹³⁸ Zentrum für Technologie und Transfer (ZTT), Worms, Germany
¹³⁹ Affiliated with an institute covered by a cooperation agreement with CERN
¹⁴⁰ Affiliated with an international laboratory covered by a cooperation agreement with CERN

^I Deceased.

^{II} Also at: Max-Planck-Institut für Physik, Munich, Germany.

^{III} Also at: Italian National Agency for New Technologies, Energy and Sustainable Economic Development (ENEA), Bologna, Italy.

^{IV} Also at: Dipartimento DET del Politecnico di Torino, Turin, Italy.

^V Also at: Department of Applied Physics, Aligarh Muslim University, Aligarh, India.

^{VI} Also at: Institute of Theoretical Physics, University of Wroclaw, Poland.

^{VII} Also at: An institution covered by a cooperation agreement with CERN.